学位論文（要約）

Magneto-rotational core-collapse supernovae

and

nucleosynthesis in extreme astrophysical environments

(磁気回転駆動型超新星爆発と極限天体環境における元素合成)

平成 28 年 12 月博士(理学) 申請

東京大学大学院理学系研究科
天文学専攻
柴垣　翔太

Abstract

Almost half of heavy nuclei beyond iron are considered to be produced by rapid neutron capture process (r-process). This process occurs in extreme astrophysical environments that satisfy high density, high temperature and high neutron-richness such as core-collapse supernovae or neutron star mergers, but the main production site is still unknown. Because there are few experimental data of neutron-rich nuclei, which are the main products in the r-process, r-process simulations are carried out with theoretical nuclear data. However, the nuclear theory is not still unified and various theoretical models on nuclear physics are suggested. This variety causes uncertainty in nucleosynthesis simulations. The astrophysical modeling is also in the similar situation. To accurately model core-collapse supernovae and binary neutron star mergers, ones need to perform high-resolution general relativistic neutrino radiation magnetohydrodynamics based on correct nuclear physics and neutrino physics. But this is computationally too heavy and practically unrealistic. Thus it is important to develop each nuclear physics model and astrophysical model step by step, and apply them to the nucleosynthesis simulations to understand how the individual development affects r-process abundances.

There has been a persistent conundrum in attempts to model the nucleosynthesis of heavy elements by the r-process. Although the locations of the abundance peaks near nuclear mass numbers 130 and 195 identify an environment of rapid neutron capture near closed nuclear shells, the abundances of elements just above and below those peaks are often underproduced by more than an order of magnitude in model calculations. At the same time, there is a debate in the literature as to what degree the r-process elements are produced in supernovae or the mergers of binary neutron stars. In the first study, we propose a novel solution to both problems. We demonstrate that the underproduction of nuclides above and below the r-process peaks in main or weak r-process models (like magnetohydrodynamic jets or neutrino-driven winds in core-collapse supernovae) can be supplemented via fission fragment distributions from the recycling of material in a neutron-rich environment such as that encountered in neutron star mergers (NSMs). In this paradigm, the abundance peaks themselves are well reproduced by a moderately neutron-rich, main r-process environment such as that encountered in the magnetohydrodynamical jets in supernovae supplemented with a high-entropy, weakly neutron-rich environment such as that encountered in the neutrino-driven-wind model to produce the lighter r-process isotopes. Moreover, we show that the relative contributions to the r-process abundances in both the solar-system and metal-poor stars from the weak, main, and fission-recycling environments required

by this proposal are consistent with estimates of the relative Galactic event rates of core-collapse supernovae for the weak and main r-process and NSMs for the fission-recycling r-process.

In the second study, we show that the result on protomagnetar wind simulations. The protomagnetar is one of the candidates for the r-process nucleosynthesis, but a long-term magnetohydrodynamic simulation for core-collapse supernovae is necessary to explore the protomanetar wind. We develop a simple, but fast computation code for this study. We carry out numerical simulations of protoneutron star winds with and without magnetic fields using an extension of an open source code, *GR1D*. This extension allows me to calculate magnetohydrodynamical evolution in a framework of 1.5 dimension. We discuss the effect of the magnetic field on the wind dynamics and nucleosynthesis.

Contents

Chapter 1

Introduction

When, where, and how were elements produced? Light elements such as hydrogen and helium were produced in the Big Bang. As the universe expands, matter cools down and collapses, and stars are formed. Fusion reactions start inside stars and synthesize elements up to iron. They are finally ejected into interstellar medium by supernova explosions. Gases polluted by heavy elements in the interstellar medium form stars again. Rich elements around us were produced in repetitions of this cycle. But heavy elements beyond iron did not appear in this story because fusion reactions to synthesize elements heavier than iron are endothermic. Then where and how were heavy elements beyond iron produced? This is one of the most important mysteries in physics and astronomy.

Instead of fusion reactions, neutron capture reactions are considered to be responsible for heavy element production (*neutron capture process*; Burbidge et al. 1957). This process is divided into two categories, i.e. slow (*s-process*) and rapid (*r-process*) neutron capture process, depending on competition between a neutron capture timescale (τ_n) and a β decay timescale (τ_β). The s-process occurs in the late phase of low-mass stars, i.e. AGB stars, where τ_n is much longer than τ_β. In this condition, nuclei that capture neutrons instantaneously undergo β decay and heavier nuclei are synthesized along the β stability line. It means that nuclear experiments can easily examine nuclei related to the s-process. On the other hand, in the r-process, τ_n is much shorter than τ_β. Nuclei continuously capture a lot of neutrons and heavy neutron-rich nuclei far from stability are formed. After all neutrons are exhausted, neutron-rich nuclei undergo β decay and finally stable nuclei are formed. In contrast to the s-process, the experimental research for the neutron-rich nuclei formed in the r-process is difficult and we have only poor knowledge on them although nuclear experiments on neutron-rich nuclei have been carried out.

Free neutrons are unstable and have a half life of about 10.2 minutes. This timescale is much shorter than stellar lives. Therefore neutrons for the neutron capture process must be supplied in situ. In the *s*-process, neutrons are formed via nuclear reactions like ^{13}C(α,n)^{16}O and ^{22}Ne(α,n)^{25}Mg*. This results in neutron number density $N_n \sim 10^7 - 10^{11}\mathrm{cm}^{-3}$. The *r*-process demands more abundant neutrons ($N_n > 10^{20}\mathrm{cm}^{-3}$). However it is difficult to establish this condition through nuclear reaction inside stars. Potential neutron sources for the *r*-process are neutrons dripping out of nuclei in high density ($> 10^{11}\mathrm{g/cm}^3$), which is established in neutron stars. Neutrons are stable for β decay due to high electron fermi energy there. Astrophysical episodes that eject neutron star material are core-collapse supernovae and binary neutron star mergers. The *r*-process is expected to take place in these astrophysical phenomena although several problems about these phenomena still remain unresolved.

In this chapter, I review current understanding of *r*-process nucleosynthesis in core-collapse supernovae and neutron star mergers as well as implications from astronomical observations.

1.1 Basics of Neutron-Capture Process

The shell structure of electrons is known well to be closely related to their stability. The stability of the noble gases can be explained by their shell closure. This kind of discussion can be applied to not only atoms but also nuclei. The number of neutrons or protons inside nuclei which corresponds to their shell closure is called *magic number*. These nuclei are relatively stable in comparison with nearby nuclei in the nuclear chart and this feature connects observational feature of heavy elements to the neutron capture processes.

The schematic paths of the *s*-process and the *r*-process are illustrated in Figure 1.1. The vertical double lines show neutron magic numbers ($N = 50, 82, 126$). Both the *s*- and *r*-process paths commonly cross these lines. As I have already mentioned above, magic nuclei are relatively stable. Therefore, the magic nuclei, i.e. nuclei with a neutron magic number are easily formed and inefficiently destructed, so that the magic nuclei are accumulated in the nucleosynthesis processes. Of course, the magic nuclei formed in the *r*-process are unstable for β decay. After the *r*-process, they undergo β decay and finally become β stable isobars†. The intersection points of the *r*-process path and the neutron magic numbers are located at $A \sim 75, 125, 190$ while the ones of the *s*-process path are located at $A \sim 88, 138, 208$. Nuclei with these mass numbers are abundantly produced in the neutron capture processes.

Figure 1.2 represents the solar system abundances of nuclides at the birth. The most stable nuclide, ^{56}Fe, forms the sharp peak (so-called iron peak). Nuclides heavier than iron show char-

*A(x,y)B means a reaction A + x $\rightarrow$ B + y.

†Any individual nuclear species is called a *nuclide*. The *isobar* means a set of nuclides with the equal mass number, but different atomic number. Likewise, the *isotope* means a set of nuclides with the equal atomic number, but different neutron number. A set of nuclides with the equal neutron number, but different atomic number is called the *isotone*. In this thesis, the word isotopes sometimes means nuclides although this is not strictly correct.

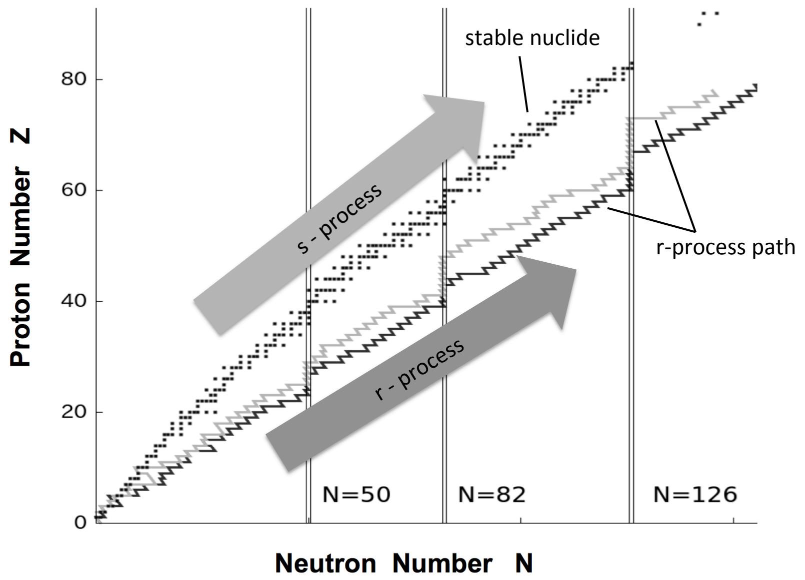

Figure 1.1: Schematic picture of neutron capture processes. The s-process synthesizes stable nuclides and their neighbors, so that the s-process proceeds along the β stability line. On the other hand, the r-process takes place far from the stability line. The vertical double lines indicate the neutron magic numbers.

acteristic three twin peaks, $(A_{low}, A_{high}) \sim (74, 88), (129, 138), (195, 208)$. Some representative nuclides in these peaks are shown in Figure 1.2. The mass numbers of these heavy element peaks correspond to the mass numbers at which paths of the neutron capture processes intersect the neutron magic numbers. Therefore, the observed solar abundances peaks are naturally interpreted as a consequence of the nuclear shell closure. The groups of abundant nuclei located at $A \sim 75, 125, 190$ are called 1st, 2nd and 3rd r-process peak, respectively while the ones at $A \sim 88, 138, 208$ are called 1st, 2nd and 3rd s-process peak, respectively.

1.2 Metal-Poor Star

Information on the r-process site can be found in metal-poor stars. As I mentioned above, heavy elements such as iron in the interstellar gas are accumulated via the stellar life cycle. Thus composition of metal-poor stars reflects ejecta composition of the individual explosive events such as supernovae that occurs in very early galaxies. Recent astronomical observations found two kind of composition in metal-poor stars. One is similar to the r-process elemental abundances in the solar system (e.g. Sneden et al. 2008), which is derived by subtracting the s-process component from the solar system composition. The other is different from the solar-system composition and has abundances with steeper decline as a function of atomic number

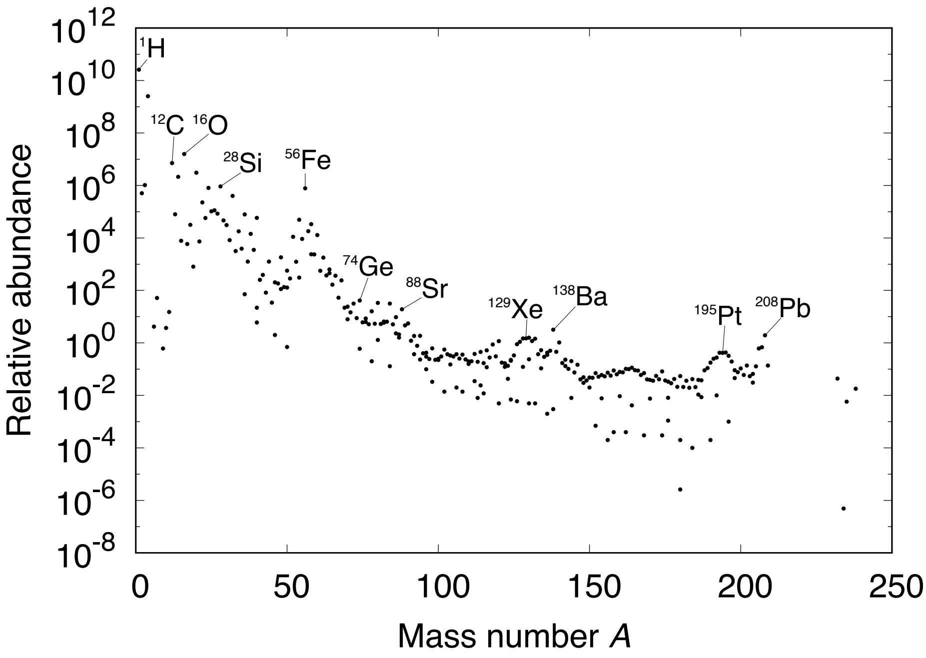

Figure 1.2: Relative abundances of nuclides in the solar system 4.56Gyr ago. The abundances are normalized to the abundance of silicon atoms (Si $= 10^6$). The abundance data are from Lodders (2010).

(Honda et al. 2004). These results indicate at least two kind of the r-process. I note that conventionally $\log\varepsilon \equiv \log_{10}(\mathrm{N_A}/\mathrm{N_H}) + 12.0$ and that $[\mathrm{A}/\mathrm{B}] \equiv \log_{10}(\mathrm{N_A}/\mathrm{N_B}) - \log_{10}(\mathrm{N_A}/\mathrm{N_B})_{\odot}$.

1.3 Astrophysical Candidates for the r-Process

A necessary condition for the r-process is neutron-rich ejecta. The neutron-rich condition is often achieved in the inside and surroundings of compact objects because the β equilibrium in the high-density circumstances favorably form neutron-rich matter as is taking place during the formation of neutron stars. The other condition for the r-process is such high density and high temperature that the nucleosynthesis process goes beyond $A = 5$ and 8 gap, i.e., 3α reaction or $\alpha\alpha n$ reaction can operate. Astrophysical phenomena which satisfy these extreme conditions are core-collapse supernovae and compact binary mergers. I describe their current understanding below.

1.3.1 Core-Collapse Supernova

Neutrino Driven Supernova

The viable candidate for the r-process site was the neutrino-driven core-collapse supernova (CCSN). A shockwave formed at the core bounce is stalled due to energy loss of photodisintegration of heavy nuclei. This stalled shock would be revived by neutrino heating emitted from a central protoneutron star. After the shock revival, material on top of the protoneutron star is continued to be heated up by neutrinos and outflow would occur. This is called neutrino-driven wind.

Woosley et al. (1994) investigated the supernova explosion and neutrino-driven wind with numerical simulations, and their neutrino-driven winds had sufficiently large entropy per baryon (> 300) and sufficiently low electron fraction (< 0.4) for the r-process. But recent numerical simulations showed that neutrino-driven winds from the proto-neutron star of the CCSN have such high electron fraction (~ 0.5) and low entropy (~ 100) that heavy r-process elements cannot be synthesized (Fischer et al. 2010; Hüdepohl et al. 2010). Also a recent simulation of an electron-capture supernova (ECSN), a CCSN of a O-Ne-Mg core progenitor, showed the possibility that ECSNe produce the light r-process element up to Cd (Wanajo et al. 2011). These results indicate the existence of the other source of the r-process elements.

Magneto-rotational Supernova

Since LeBlanc & Wilson (1970), the magnetorotaional mechanism that drives core-collapse supernova explosions has been studied. The rotational winding of the magnetic field lines works like a spring and forms jets along the rotational axis, so that the neutron-rich matter near the protoneutron star surface are quickly carried outward by the magnetic spring. This mechanism can avoid the neutrino interaction, which transforms neutrons to protons. Numerical fluid simulations and post-process nucleosynthesis simulations for magnetorotational supernovae (Nishimura et al. 2006; Fujimoto et al. 2007, 2008; Winteler et al. 2012; Nishimura et al. 2015) show that magnetorotational supernovae can produce r-process elements, and higher initial angular velocity and higher initial magnetic field lead to the production of heavier r-process elements. A 3D fluid instability may affect jet evolution (Mösta et al. 2014a) and magnetorotational instability may play an important role in the post bounce evolution (Sawai & Yamada 2014), but these effects are still under debate.

1.3.2 Compact Binary Merger

The compact binary merger scenario is first proposed by Lattimer & Schramm (1974, 1976) for black hole-neutron star mergers and by Eichler et al. (1989) for neutron star-neutron star mergers. Recent simulations of r-process nucleosynthesis in neutron star mergers showed that the 2nd and 3rd r-process peaks in the solar-system composition are reproduced well but light neutron-capture elements are not produced due to highly neutron-rich ejecta (their electron fraction < 0.1)(Goriely et al. 2011; Korobkin et al. 2012). More recently, Wanajo et al. (2014)

and Goriely et al. (2015) show a large impact of weak interaction on the electron fraction of binary neutron star mergers (~ 0.3). As a result, Wanajo et al. (2014) present that the fully general relativistic simulation with neutrino transfer for binary neutron star merger reproduces a whole of r-process elements. However, Radice et al. (2016) show conventional neutron-rich ejecta (electron fraction ~ 0.1) from the neutron star merger in their numerical relativity simulation with radiation transfer. So ones still need development of them to obtain the clear conclusion on the neutron star merger. In contrast to binary neutron star mergers, black hole-neutron star mergers release very neutron-rich material due to tidal disruption, so that only heavy r-process elements are synthesized (Just et al. 2015).

Radioactive decays of freshly synthesized unstable nuclei in compact binary merger events should heat up the expanding material, which is similar to the gamma-ray heaing by the radioactive decay of iron-group elements just after the supernova explosion, and electromagnetic transients appear. This scenario is firstly suggested by Li & Paczyński (1998). This phenomenon is called macronova (Kulkarni 2005) or kilonova (Metzger et al. 2010). This hypothesis has been payed attention to since the first discovery of an infrared excess in an afterglow associated with a short gamma-ray burst, GRB 130603B (Tanvir et al. 2013). Later, it was reported that GRB 060614 also showed an infrared excess in its afterglow (Yang et al. 2015; Jin et al. 2015). Kasen et al. (2013) and Tanaka & Hotokezaka (2013) explored the macronova/kilonova in radiative transfer simulations and concluded that r-process products have higher opacity ($\sim 10\ \mathrm{cm^2 g^{-1}}$) than supernovae ($\sim 0.1\ \mathrm{cm^2 g^{-1}}$), so that their brightening is dimmer.

1.4 Nuclear Physics Uncertainty

Uncertainty of nuclear physics is also important for numerical simulations of r-process nucleosynthesis. As I mentioned above, ones do not have experimental data on neutron-rich nuclei. Thus we usually use a theoretical nuclear model including neutron-rich nuclei to calculate the r-process simulation. But there are many models and their difference can affect the r-process simulation. For example, Arcones & Martínez-Pinedo (2011) investigate the dependence of the r-process nucleaosynthesis on nuclear mass models. Korobkin et al. (2012) and Eichler et al. (2015) also explore the effect of the fission fragment mass distributions on the resulting elemental abundances for binary neutron star mergers. Mumpower et al. (2016) explore sensitivity of nuclear physics input to the r-process nucleosynthesis by changing a huge amount of nuclear reactions and reveal the critical reactions for the r-process abundances. Sasaqui et al. (2005) focus on uncertainty of the light-element reactions and explore their sensitivity of light nuclear reactions to the r-process. To pin down the nuclear uncertainty, the nuclear experiment plays a key role (e.g. Lorusso et al. 2015).

1.5 Plan of This Thesis

This thesis deals with two topics related to nucleosynthesis of magneto-rotational supernovae: 1. an underproduction problem of r-process elements in magneto-rotational supernovae (Chapter 3); 2. elemental abundances of magnetized protoneutron star winds blown out after magneto-rotational supernovae (Chapter 4). Note that, in Chpater 2, I describe our nuclear reaction network code, used in later chapters; and in Chapter 5, I summarize this thesis.

Chapter 2

Nuclear Reaction Network Code

We will discuss results of nucleosynthesis in the latter two chapters. For preparation, we describe contents and structure of our nuclear reaction network code in this chapter.

2.1 Basic Equation

2.1.1 Nuclear Statistical Equilibrium

At $T_9(\equiv T/10^9[K]) > 9.0$, arbitrary nuclei are in equilibrium of the following reactions:

$$(Z, A) + p \quad \leftrightarrow \quad (Z+1, A+1) + \gamma, \tag{2.1}$$

$$(Z, A) + n \quad \leftrightarrow \quad (Z, A+1) + \gamma, \tag{2.2}$$

where (Z, A) is a nucleus with atomic number Z and mass number A. This state is called nuclear statistical equilibrium (NSE). Then we can write the chemical potential of the nucleus, $\mu(Z, A)$, with those of proton and neutron, μ_p, μ_n:

$$\mu(Z, A) = Z\mu_p + (A-Z)\mu_n. \tag{2.3}$$

If we assume an ideal nonrelativistic Maxwell-Boltzmann gas, the elemental abundance is written as

$$Y(Z, A) = \frac{G(Z, A)A^{3/2}}{2^A}\left(\frac{2\pi\hbar^2}{m_\mu kT}\right)^{3(A-1)/2}\left(\frac{\rho}{m_\mu}\right)^{A-1} Y_n^{A-Z} Y_p^Z \exp\left(\frac{B(Z, A)}{kT}\right), \tag{2.4}$$

where

$$Y(Z, A) = \frac{n(Z, A)}{\rho N_A} \tag{2.5}$$

is the yield of the nucleus (Z, A), $G(Z, A)$ is the nuclear partition function, m_μ is atomic mass unit,

$$B(Z, A) = c^2[Zm_p + (A - Z)m_n - M(Z, A)] \tag{2.6}$$

is the nuclear binding energy and $M(Z, A)$ is the mass of the nucleus (Z, A).

To specify Y_p and Y_n, we use charge and baryon conservation:

$$Y_e = \sum_{(Z,A)} ZY(Z, A), \tag{2.7}$$

$$\sum_{(Z,A)} AY(Z, A) = 1. \tag{2.8}$$

Therefore we can determine the composition in NSE from ρ, T and Y_e. Our nucleosynthesis calculations start from T_9=9.0, where NSE is satisfied. The initial composition is determined via eq. (2.4) (2.7) (2.8) with ρ and Y_e at $T_9 = 9.0$.

2.1.2 Abundance Evolution

The equations of nuclear abundance evolution for isotope i in a Lagrangian formulation are

$$\frac{dY_i}{dt} = \sum_{\substack{a\cdots,b,\\ c,\cdots,d}} \lambda^{i,a,\cdots,b}_{c,\cdots,d} Y_c \cdots Y_d - \sum_{\substack{a,\cdots,b,\\ c,\cdots,d}} \lambda^{c,\cdots,d}_{i,a,\cdots,b} Y_i Y_a \cdots Y_b, \tag{2.9}$$

where $\lambda^{i,a,\cdots,b}_{c,\cdots,d}$ and $\lambda^{c,\cdots,d}_{i,a,\cdots,b}$ are the reverse and forward nuclear reaction rates of the following reaction:

$$i + a + \cdots + b \leftrightarrow c + \cdots + d, \tag{2.10}$$

respectively.

We can write the set of ordinary differential equations (2.9) in the more compact form

$$\frac{dy_i}{dt} = f_i(y_j). \tag{2.11}$$

We apply a semi-implicit first-order Euler method for numerically integrating eq. (2.11). When it is applied to the equations, eq. (2.11) is written in the following equation:

$$\sum_j \left(\frac{\delta_{ij}}{\Delta t^{(k)}} - \frac{\partial f_i}{\partial y_j} \right) \delta y_j^{(k)} = f_i(y_j^{(k)}), \tag{2.12}$$

where $\Delta t^{(k)}$ is the kth time step and $\delta y_j^{(k)}$ is the difference between the abundance of isotope j at kth step and that at $(k+1)$th step. This equation is simply the matrix equation $A\mathbf{x} = \mathbf{b}$. Thus it can be solved by an upper triangularization via a Gaussian elimination and a back substitution.

2.2 Nuclear Data Set

Our nuclear reaction network code is based on Terasawa et al. (2001) and covers a range of nuclei from proton and neutron to nuclei with $Z = 114$ and from experimentally known stable nuclei to theoretically predicted unstable neutron-rich nuclei. The nuclear data are based on the experimental data whenever possible. Otherwise, we use the theoretical data as described below. The neutron capture cross sections in Cowan et al. (1991) are used. The nuclear masses are taken from Koura et al. (2005, KTUY05). The β-decay rates, the β-delayed neutron emission probabilities and the β-delayed fission rates are taken from Chiba et al. (2008). The spontaneous fission rates and the α-decay rates in Koura (2004) are used. The β-delayed fission reaction is the most dominant fission mode. So here the other fission modes such as the neutron-induced fission are not included in our code for simplicity (see Figure 1 in Chiba et al. (2008)). We will mention our fission model in more detail in Chapter 3.

The reverse reactions rate for i(j,o)m, i.e the reaction rate for m(o,j)i, is calculated by

$$N_A < \sigma v >_{m+o} = \left(\frac{A_i A_j}{A_o A_m}\right)^{3/2} \frac{(2J_i+1)(2J_j+1)}{(2J_o+1)(2J_m+1)} \frac{G_i}{G_m} e^{-Q/kT} N_A < \sigma v >_{i+j}, \qquad (2.13)$$

where N_A is Avogadro number, J and A are spins and masses, G is partition functions and Q is a Q value for this reaction. The reverse reaction rate of a radiative capture reaction i(j,γ)m, λ_γ is calculated from the capture rate as follows:

$$\lambda_\gamma = 9.8685 \times 10^9 T_9^{3/2} \left(\frac{A_i A_j}{A_m}\right)^{3/2} \frac{(2J_i+1)(2J_j+1)}{(2J_m+1)} \frac{G_i}{G_m} e^{-Q/kT} N_A < \sigma v >_{i+j} . \qquad (2.14)$$

2.3 Numerical Implementation

First of all, it is noted that index i in eq. (2.11) is first in the order of isotopes from stable to neutron-rich nuclei and second in the ascending order of atomic number like $\cdots$, (Z, A), $(Z, A+1)$, $\cdots$, $(Z+1, A')$, $\cdots$. The six light nuclei of neutron, proton, deuterium, tritium, helium-3 and helum-4 are exceptional. These nuclei are set to the highest indexes.

First let us consider a nuclear reaction network code without fission processes. The Jacobian matrix in eq. (2.11) is mainly composed of diagonal matrix elements and their neighbors as shown in the left panel of Figure 2.1. Matrix elements involved with light nuclei shown at the bottom and right edge of the Jacobian matrix are rather dense. This structure allows us to save memory and to use smaller loops for an upper triangularization in numerical simulations by avoiding to store zero matrix elements. The righthand panel of Figure 2.1 represents how to store the Jacobian matrix in our code. Our code decomposes the Jacobian matrix into 4 small matrices (or arrays). The diagonal part is stored in a non-square matrix (array). The array to store the diagonal part is horizontally taken to be in a larger size (M) than the width of the diagonal part (m) because this array is also used for triangularization. But the total size M is still much smaller than the original matrix size (N), so this method is still quite efficient.

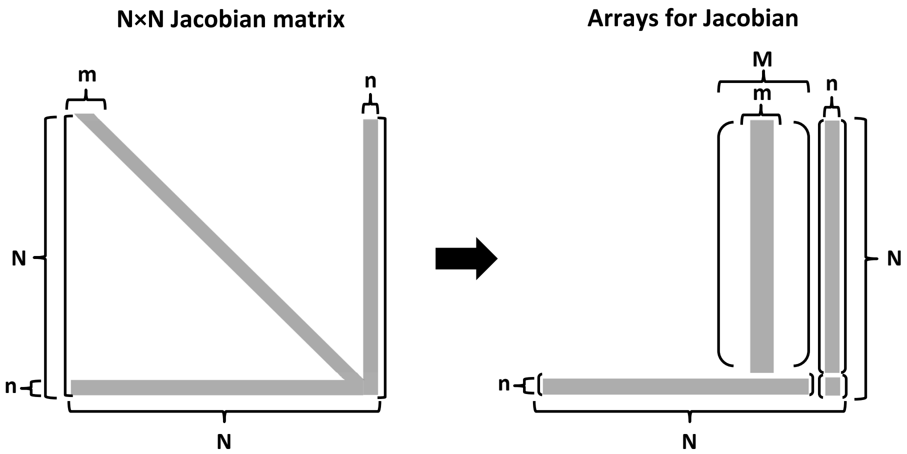

Figure 2.1: Schematic picture of a Jacobian matrix that arises in nucleosynthesis simulations *without fission* (Left) and arrays that efficiently store the nonzero Jacobian matrix elements in our code (Right). Gray parts represent nonzero matrix parts and white parts represent zero matrix parts.

Next let us consider a nuclear reaction network code including fission processes. In this case, the Jacobian matrix in eq. (2.11) is composed of the fission contribution that arises far from the diagonal part and the same as previous matrix parts as shown in the left panel of Figure 2.2. The easiest way to include the fission contribution in our nuclear reaction network code is to take larger M so that the small matrix (or array) for the diagonal part can cover the fission part in the Jacobian matrix. However, this treatment clearly causes inefficient calculations because the M×N-n small matrix contains a large number of zero elements. To avoid this, our new code decomposes the Jacobian matrix into 4+1 small matrices (or arrays) as shown in the right panel of Figure 2.2. The additional small matrix (or array) stores fission contribution. This method keeps advantages of the original code that small M is possible, and actually reduces zero elements stored in the matrices (or arrays) in comparison with the easiest way described above.

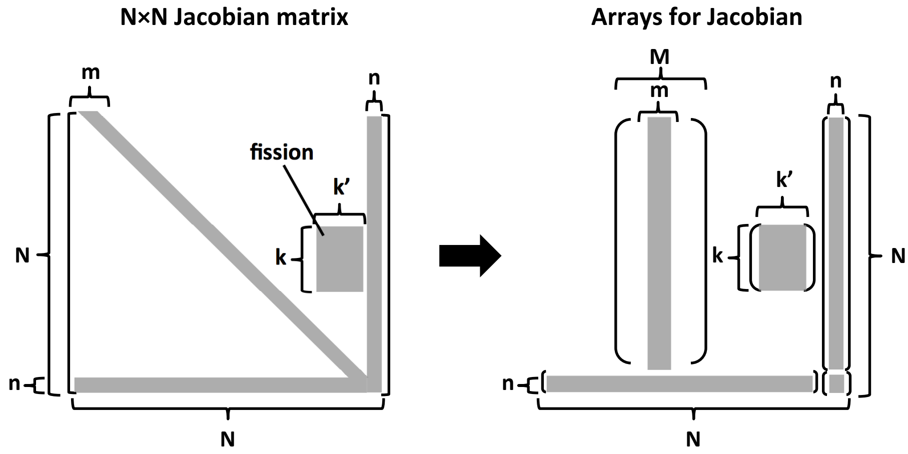

Figure 2.2: Schematic picture of a Jacobian matrix that arises in nucleosynthesis simulations *including fission* (Left) and arrays that efficiently store the nonzero Jacobian matrix elements in our code (Right). Gray parts represent nonzero matrix parts and white parts represent zero matrix parts. The additional array is used to store the nonzero matrix elements that nuclear fission makes.

Chapter 3

Relative Contributions of the Weak, Main and Fission-Recycling r-Process*

3.1 Introduction

It has been known for more than half a century (Burbidge et al. 1957) that about half of the elements heavier than iron are produced via rapid neutron capture (the r-process). Indeed, the basic physical conditions for the r-process are well constrained (Burbidge et al. 1957) by simple nuclear physics. The observed abundance distribution requires a sequence of near equilibrium rapid neutron captures and photoneutron emission reactions far on the neutron-rich side of stability. This equilibrium is established with a maximum abundance strongly peaked on one or two isotopes far from stability. The relative abundance of r-process elements is then determined by the relative β-decay rates along this r-process path., i.e., longer β-decay lifetimes result in higher abundances.

In spite of this simplicity, however, the unambiguous identification of the site for the r-process nucleosynthesis has remained elusive. Parametrically, one can divide current models for the r-process into three scenarios roughly characterized by the number of neutron captures per seed nucleus (n/s). This parameter, in turn is the consequence of a variety of conditions such as time-scale, baryon density, average charge per baryon, $Y_e \equiv \langle Z/A \rangle$, and entropy (or baryon to photon ratio) corresponding to different astrophysical environments (e.g. Meyer & Brown 1997;

*Contents of this chapter are based on the article " Relative Contributions of the Weak, Main, and Fission-recycling r-process ", Shibagaki, S., Kajino, T., Mathews, G. J., Chiba, S., Nishimura, S., Lorusso, G., Astrophysical Journal, 816, 79, (2016).

Otsuki et al. 2003).

An environment in which there are few neutron captures per seed ($n/s \sim 50$) produces what has been identified as the weak r-process (Wasserburg et al. 1996). It can only produce the lightest r-process nuclei up to $A \sim 125$. Such an environment may occur, for example, in the neutrino-driven wind of core-collapse supernovae (CCSNe) (Woosley et al. 1994; Wanajo 2013), part of the outflow from the remnant of compact binary mergers (Rosswog et al. 2014; Perego et al. 2014; Just et al. 2015), the delayed magnetohydrodynamic (MHD) jet from CCSNe (Nishimura et al. 2015).

An environment with enough neutron captures per seed ($n/s \sim 100$) to produce the two r-process abundance peaks at $A = 130$ and 195 corresponds to what has been dubbed the main r-process and could correspond, for example, to the ejection of neutron-rich material via magnetic turbulence in magnetohydrodynamically driven jets (MHDJ) from core collapse supernovae (Nishimura et al. 2006; Fujimoto et al. 2007, 2008; Ono et al. 2012; Winteler et al. 2012; Nakamura et al. 2015; Nishimura et al. 2015), or in neutron star mergers (NSMs) (Wanajo et al. 2014; Goriely et al. 2015).

In this study, we are particularly interested in a third environment that we dub the fission-recycling r-process. In this environment the number of neutron captures per seed nucleus can be very large ($n/s \sim 1000$). The r-process path then proceeds along the neutron drip line all the way to the region of fissile nuclei ($A \approx 300$) where the r-process is terminated by beta- or neutron-induced fission. Fission recycling can then occur whereby the fission fragments continue to experience neutron captures until beta- or neutron-induced fission again terminates the r-process path. After a few cycles the abundances can become dominated by the fission fragment distributions and not as much by the beta-decay flow near the closed shells. Hence, a very different mass distribution can ensue. Such environments are often associated with the dynamical ejecta from NSMs in which the tidal ejection of neutron-rich material during the merger can lead to fission recycling and many neutron captures per seed (e.g. Goriely et al. 2011; Korobkin et al. 2012; Piran et al. 2013; Rosswog et al. 2013; Goriely et al. 2013).

Observations (Sneden et al. 2008) showing the appearance of heavy-element r-process abundances early in the history of the Galaxy seem to favor the short progenitor lifetime of CCSNe over NSMs as the r-process site. However, identifying the r-process site in models of CCSNe has been difficult (Arnould et al. 2007; Thielemann et al. 2011).

The three types of environments, neutrino-driven winds (NDWs), magnetohydrodynamic jets (MHDJs), and neutron star mergers (NSMs), have all been studied extensively in the recent literature. The robustness of the results varies for different environments, but uncertainties in both astrophysical conditions and nuclear input are well recognized in all cases. For example, the previously popular model (Woosley et al. 1994) of r-process nucleosynthesis in the NDW above the newly forming neutron star has been shown (Fischer et al. 2010; Hüdepohl et al. 2010) to be inadequate as a main r-process site when modern neutrino transport methods have been employed. The required neutron captures per seed do not occur in the neutrino energized wind. Nevertheless, it is quite likely that the weak r-process does occur (Wanajo 2013) in the NDW producing neutron rich nuclei up to about $A \sim 125$.

Regarding the weak r-process, however, one should note that while most s-process models now produce r-process residuals for $A \gtrsim 120$ which look remarkably similar, this is not the case for lighter nuclei. Hence, there is some uncertainty in determining the solar-system r-process abundances via subtraction of the s-process contribution from the total abundances. Indeed, a final consensus has not yet been reached on the predicted s-process abundances of light elements. Hence, what is usually taken to be the weak r-process [or unknown lighter element primary process (LEPP)] may actually correspond to a much different environment. For example in Trippella et al. (2014) it was demonstrated that enhanced light-element abundances could arise via non-parametric MHD-driven mixing mechanisms. This enhanced light-element s-process component could obfuscate the need for a weak r-process. Nevertheless, with this *caveat* in mind we adopt the NDW in supernovae as representative of the weak r-process. We note, however, that our arguments below regarding the relative contribution of the weak r-process may in fact refer to the relative contribution of an s-process driven LEPP.

Indeed, the difficulties in reproducing the r-process abundances have motivated many new studies of NSMs (e.g. Goriely et al. 2011; Korobkin et al. 2012; Goriely et al. 2013; Wanajo et al. 2014; Perego et al. 2014). Nevertheless, one scenario for the r-process in CCSNe remains viable. It is the MHDJ model (Nishimura et al. 2006; Fujimoto et al. 2007, 2008; Ono et al. 2012; Winteler et al. 2012; Nakamura et al. 2013, 2015; Nishimura et al. 2015). In this model magnetic turbulence leads to the ejection of neutron rich material into a jet. As the jet transports this neutron-rich material away from the star it can undergo r-process nucleosynthesis in a way that avoids the low neutron-to-seed ratios associated with neutrino interactions in the NDW model. Moreover, the required conditions of the r-process environment (timescale, neutron density, temperature, entropy, electron fraction, etc.) are well accommodated in this model.

However, there is a persistent problem in this model, or any general model (e.g. Meyer & Brown 1997; Otsuki et al. 2003) in which the r-process elements are produced in a short time scale via the rapid expansion of material away from a neutron star. In such models, the neutron density rapidly diminishes and r-process path freezes out near the neutron closed shells far from stability. Most such models underproduce isotopic abundances just below and above the r-process abundance peaks as we describe in more detail below.

Indeed, all r-process models are fraught with uncertainties in the input nuclear physics, the astrophysical environment, and the galactic chemical evolution. Rather than to give up, however, it is highly desirable to explore any possible method in which the relative contributions of each of the primary environments (weak, main, and fission recycling) could be ascertained from observation. In this study we propose such a possibility.

With this in mind our goal is to analyze the general advantages and disadvantages of each of the characteristic environments. Although we have noted here specific astrophysical models that are likely to be associated with the various conditions, the readers should be aware of the uncertainties involved and consider these environments as illustrative, not definitive. Nevertheless, we speculate here that it may be possible to quantify the relative contribution of each scenario to the observed solar-system r-process abundance distribution and the distribution of r-process elements in the early Galaxy. The novel conclusion of this study is that one can possibly utilize the inherent shortcomings of the three characteristic environments to estimate the relative contributions of each (weak, main, and fission recycling) to the final observed r-process abundances.

3.2 Effect of Nuclear Closed Shells

Figure 3.1 illustrates why the abundances below and above the r-process peaks are bypassed. It shows an example of a typical calculated r-process path near the $N = 82$ neutron closed shell just before freezeout when the neutrons are rapidly exhausted and the abundances begin to beta decay back to the region of stable isotopes. Neutron captures and photo-neutron emission proceed in equilibrium for nuclei with a neutron binding energy of about 1-2 MeV. Above and below a closed neutron shell, however, this r-process path shifts abruptly toward the closed shell from below (or away from the closed shell for higher nuclear masses). This shifting of the r-process path toward the $N = 82$ neutron closed shell causes isotopes with $N = 70 - 80$ ($A \sim$110-120) to be bypassed. Similarly, the $A =$140-147 underproduction corresponds to the isotopes with proton closed shell $Z = 50$ and $N \sim$90-97 ($A \sim$140-147). These isotopes will also be bypassed in the beta-decay flow as is evident on Figure 3.1.

I emphasize that this is not just an artifact of the particular mass model employed in this study. Nearly all models in the current literature with a rapid freezeout (including the MHDJ; Nishimura et al. 2006; Fujimoto et al. 2007, 2008; Ono et al. 2012; Winteler et al. 2012; Nakamura et al. 2013; Nishimura et al. 2015) show this underproduction if the final abundances are normalized to the abundance peaks. Indeed, one is hard pressed to find any model for the main r-process (including NDW models) in which this underproduction does not occur.

One can of course contrive calculations to somewhat fill the dips on both sides of the second r-abundance peak. Recently, for example, Lorusso et al. (2015) were able to avoid the underproduction in a schematic high-entropy outflow model by incorporating a summation of several entropies. In such a model one can fill in the dips similarly to the way we propose to do this by summing contributions from various physical conditions. As another example, calculations could fill the dips by using the ETFSI mass model as displayed in Fig. 7 in Nishimura et al. (2006)). However, these models do so at the cost of displacing the 2nd and 3rd peaks and/or underproducing (or overproducing) abundances over a wide mass region between the second and third peaks. This was also a consistent feature in the original realistic NDW models of Woosley et al. (1994). Indeed this effect is apparent in almost every r-process calculation since the 1970s (cf. review in Mathews & Ward 1985).

I note, however, that new attempts have been presented (Kratz et al. 2014) of r-process calculations in a parameterized NDW scenario based upon the models of Freiburghaus et al. (1999). Making use of new nuclear masses and beta-decay rates from the finite-range droplet model FRDM (2012) (Möller et al. 2012) it was shown that the previous discrepancies near $A = 120$ are significantly diminished compared to the same calculation based upon the previous FRDM(1992) (Möller et al. 1995) nuclear properties. Hence, one must keep in mind that at least some of the apparent discrepancy may be due to the adopted nuclear input.

Although it has been speculated for some time (e.g. Woosley et al. 1994; Pfeiffer et al. 2001; Farouqi et al. 2010) that this could be due to quenching of the strength of the shell closure or beta-decay rates near the closed neutron shell, this explanation is unlikely. Recent r-process calculations (Nishimura et al. 2012) based upon new measurements (Nishimura et al. 2011) of beta-decay half lives near the A =130 r-process path have confirmed the absence of shell quenching effects in the beta flow. Moreover, recently the first ever studies (Watanabe et al. 2013) of the level structure of the waiting-point nucleus ^{128}Pd (Z =46, N =82 in Fig. 1) and ^{126}Pd have been completed. This study clearly indicates that the shell closure at the neutron number N =82 is fairly robust. Hence, there is absolutely no evidence of the hypothesized quenching effects in either the beta decay rates or nuclear masses. One must suppose that some other resolution of this underproduction is necessary.

One goal of this study is, therefore, to point out that a solution to the underproduction of nuclei above and below the r-process abundance peaks can be obtained if one considers that a fission recycling environment (e.g. NSMs) has contributed to the solar-system r-process abundance distribution in addition to the environments responsible for the weak and main r-process (like CCSNe). Indeed, this novel solution not only resolves this dilemma but can *quantify* the answer to the question of the relative contributions to the r-process abundances of the weak and main r-process environments (such as those due to CCSNe) vs. long-duration fission-recycling environments (such as NSMs) .

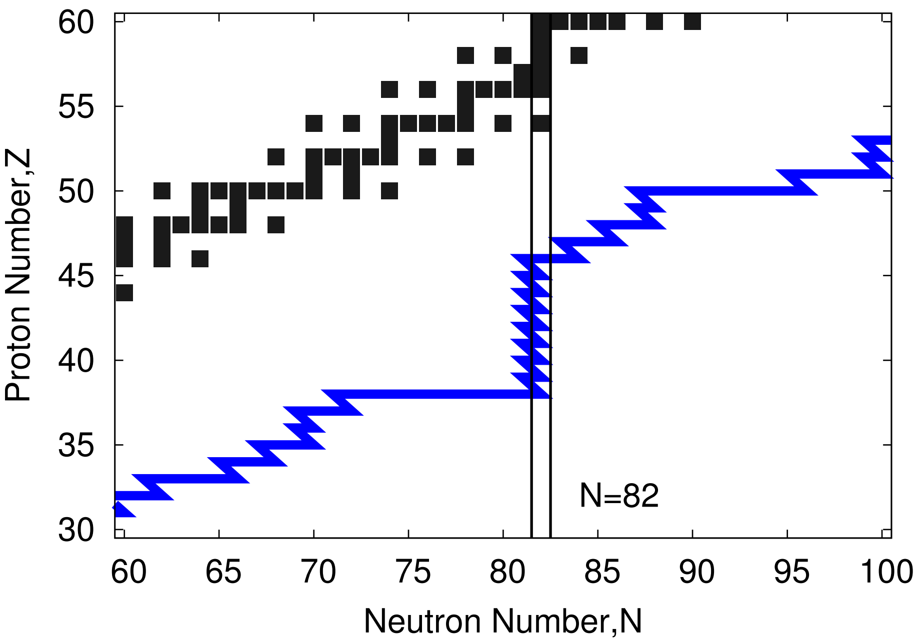

Figure 3.1: (Color online) Illustration of the (N,Z) path of r-process nucleosynthesis (blue line) for nuclei with $A \sim 90 - 150$ in the vicinity of the $N = 82$ neutron closed shell and Z=50 proton closed shell just before freezeout of the abundances in a typical main r-process (MHDJ) model. Black squares show the stable isotopes.

3.3 Fission Recycling r-Process

For this study we highlight the possible role of fission recycling to account for the underproduction problem above and below the r-process peaks often found in models for the main r-process abundances. For our purposes we employ a specific NSM model although we note that this is illustrative of any fission-recycling r-process environment. Nevertheless, the most natural current site for such fission recycling to occur is in the NSM models. The ejected matter from NSMs is very neutron-rich ($Y_e \sim 0.1$). This means that the r-process path proceeds along the neutron drip line all the way to the onset of fission recycling. As noted above, after a few cycles the abundances can become dominated by the fission fragment distributions and not as much by the beta-decay flow near the closed shells. Hence, a very different mass distribution can ensue.

In this regard we note that a number of recent studies (Goriely et al. 2011; Korobkin et al. 2012; Goriely et al. 2013; Wanajo et al. 2014; Perego et al. 2014) have indicated that the r-process in NSMs can involve a distribution of neutron-rich environments. Such models can produce a final abundance pattern that is similar to the solar-system r-abundances. Here, even though we use the term NSM model, it is intended to refer to the portion of the ejecta that experiences fission recycling, while the other ejecta is similar to a NDW or MHDJ like model. Hence, when we refer to the NSM model we really mean the ejecta that experiences fission recycling that fills in the bypassed abundances produced in trajectories that produce the main r-process.

An important point is that models including fission recycling effects produce a final abundance pattern that is relatively insensitive to the astrophysical uncertainties (Korobkin et al. 2012), although the total (including non-recycling ejecta) abundances can be sensitive to the detailed model.

Nevertheless, the distribution of nuclear fission products can affect the abundance pattern. Hence, one must carefully extrapolate fission fragment distributions (FFDs) to the vicinity of the r-process path (cf. Martínez-Pinedo et al. 2007; Erler et al. 2012). We argue that by incorporating the expected broad distribution of fission fragments based upon phenomenological fits to observed FFDs, the effect of the neutron closed shells becomes smoothed out, thereby providing a means to fill in the isotopes bypassed in the main r-process.

For the present study we have made use of self consistent β-decay rates, β-delayed neutron emission probabilities, and β-delayed fission probabilities taken from Chiba et al. (2008). The spontaneous fission rates and the α-decay rates are taken from Koura (2004). In our r-process calculations, β-delayed fission is the dominant nuclear fission mode. Hence, for the most part other fission modes like neutron-induced fission can be neglected (Chiba et al. 2008).

To generate FFDs far from stability we have made use of a semi-empirical model (Ohta et al. 2008; Tatsuda et al. 2008; Chiba et al. 2008) that well reproduces the systematics of known fission fragment distributions. This model can be naturally extrapolated to the required heavy neutron rich isotopes of the r-process. As such it is a robust alternative means to predict yields from fission recycling.

A key ingredient of this model is that it can account for FFDs that can either be single humped, bimodal or even trimodal. This is achieved by a weighted superposition of up to three Gaussian functions:

$$f(A, A_p) = \sum_{A_i} \frac{1}{\sqrt{2\pi}\sigma} W_i \exp\left(\frac{-(A - A_i)^2}{2\sigma^2}\right) \ , \tag{3.1}$$

where A is the mass number of each fission fragment, A_p is that of the parent nucleus, σ is the width of the three Gaussian functions, and the sum is over the possible fission fragment distributions, $i = L, H, M$, with

$$A_H = \frac{(1+\alpha)}{2}(A_p - N_{loss}) \quad , \tag{3.2}$$

$$A_L = \frac{(1-\alpha)}{2}(A_p - N_{loss}) \quad , \tag{3.3}$$

and

$$A_M = \frac{(A_H + A_L)}{2} \quad . \tag{3.4}$$

The factor W_i is a weighting given by $(1 - \omega_s)$ for $i = L, H$ and $2\omega_s$ for $i = M$. The quantities ω_s and α are shape symmetry and mass-asymmetry parameters, respectively as defined below. N_{loss} is the number of prompt neutrons.

For the present application we include the dispersion in the FFDs ($\sigma = 7.0$) and $N_{loss} = 2$ from measured experiments on actinides. The adopted fission neutron emission is an average value for all possible fission events. We have run calculations in which this number N_{loss} is varied from 2 to 8 and found that the results are nearly indistinguishable although a very small change is found below $A < 100$ and near the valley around $A = 180$. The atomic number and neutron number of each fission fragment is determined by the assumption that the proton to neutron number ratio is the same as that of the parent nucleus after correcting for prompt neutron emission, i.e. $Z_p/N_p = Z/(N + N_{loss}/2)$.

I have run calculations in which Gaussian width parameter σ is varied from 4 to 14 and compared with the result with $\sigma = 7$. We found that the rare-earth peak changes by only +20%,-25% so that the abundance decreases slightly for larger σ. Although the abundances below $A < 100$ and near the valley around $A = 180$ increases as σ increases, these changes do not change the overall distribution drastically, and the conclusions of this article are not affected by fixing $\sigma = 7$.

The quantity α in Eqs. (2) and (3) is the average mass-asymmetry parameter corresponding to the valley of the potential energy surface of the parent nucleus near the scission point for nuclear fission. This has been calculated in the liquid drop model (Myers & ŚwiaŢecki 1999) with shell energy corrections determined (Iwamoto et al. 1976; Sato et al. 1979) from the two-center shell model in the three-dimensional shape parameter space comprised of α, the distance between the centers of the two-harmonic oscillators z, and the deformation parameter of the fission fragments, δ. The quantity ω_s is determined as $\omega_s = -0.2(V_s - V_a - 2.0)$ for $V_s - V_a < 2.0$ MeV, and $\omega_s = 0$ otherwise, where V_s and V_a denote the potential values at symmetric and asymmetric valleys, respectively, at the fragment distance z corresponding to scission. This approximate formula is derived to account for the observed rapid change between asymmetric-and symmetric-mass distributions around ^{256}Fm, i.e. V_s is adjusted relative to V_a to reproduce the observed mass distributions of the Fm isotopes with Eq. (1).

For illustration in the present study we have carried out r-process simulations in the fission recycling environment from the NSM outflow models of Korobkin et al. (2012); Piran et al. (2013); Rosswog et al. (2013). As an illustration of the main r-process we take abundances in the ejecta from the MHDJ model of Nishimura et al. (2012). For the weak r-process we use yields from the NDW models of Wanajo (2013).

Our adopted NSM outflow model is derived from 3D Newtonian smoothed-particle hydrodynamics (SPH) (Korobkin et al. 2012; Piran et al. 2013; Rosswog et al. 2013). It gives qualitatively similar results to the fission recycling r-process yields calculated in 3D general relativistic SPH simulations (Bauswein et al. 2013; Goriely et al. 2013) and the full 3D general relativistic simulations of (Wanajo et al. 2014) in the heavier mass region. The details are different for lighter masses because of the broader range of neutron densities and electron fractions in the particle trajectories in those models.

We emphasize that the models run here can be considered as generic fission recycling models. For specific NSM models we utilize the trajectories from the binary neutron star merger of two neutron stars with $M = 1.0$ $M_\odot$ each. Although 1.0 $M_\odot$ is not the typical neutron star mass (Valentim et al. 2011), it has been shown (Korobkin et al. 2012) that the resulting abundances are nearly independent of the neutron star masses in the binary. The hydrodynamic simulations are based upon the SPH method of Rosswog (2009), the equation of state (EoS) of Shen et al. (1998a,b), an opacity-dependent multi-flavor neutrino leakage scheme (Rosswog & Liebendörfer 2003), and Newtonian gravity. We use 30 available trajectories of neutron star merger ejecta to calculate the nucleosynthesis[†]. The ejected mass from this binary merger is ~ 0.01 $M_\odot$ (Korobkin et al. 2012). After the end of the hydrodynamic simulation at $t_{\rm fin}(\sim 15$ ms) the thermodynamic evolution can be continued (Rosswog et al. 2014) as a free adiabatic expansion.

The reason for the use of these trajectories is that they are publicly available and lead to robust fission recycling. Moreover, a main point of this study is the importance of a fraction of r-process material that involves fission recycling. If some fraction of the ejects in the NSM calculations as in Goriely et al. (2011); Korobkin et al. (2012); Goriely et al. (2013); Wanajo et al. (2014); Perego et al. (2014) do not involve fission recycling, then this study deals with the fraction of material in their models that leads to fission recycling, while the other trajectories would be absorbed into what we label as other components.

In contrast to CCSNe, baryons participating in the r-process constitute a large fraction of the total mass-energy in the NSM ejecta. Thus, the nuclear energy released by the r-process

[†]Trajectories from http://compact-merger.astro su.se/

nuclear reactions must be included after $t_{\rm fin}$ by an entropy source term,

$$dS = -\epsilon_{\rm th} \sum_i \left(m_i c^2 / k_B T + \mu_i / k_B T \right) dY_i \ , \tag{3.5}$$

where a heating efficiency parameter $\epsilon_{\rm th} \approx 1$ is introduced (Korobkin et al. 2012) to account for neutrino energy losses.

The nucleosynthesis calculations were started at a temperature $T = 9.0 \times 10^9$ K. At this point all nuclei are in nuclear statistical equilibrium, and the composition is completely determined from the density and charge-per-baryon Y_e of the material ejected from the neutron stars. At this point the material almost entirely consists of free neutrons plus some heavy seed nuclei with A≈70.

As the temperature and density decrease, however, the material is evolved using an updated version of the nuclear network code of Terasawa et al. (2001). The neutron radiative capture rates are as summarized in Terasawa et al. (2001), however, for both the weak and main hot r-process considered here, the abundance patterns mainly depend on the nuclear masses and beta-decay rates but not on the radiative neutron-capture rates. This is because the system proceeds in (n, γ) equilibrium until a rapid freezeout of the neutron abundance. On the other hand, the fission-recycling NSM r-process considered here depends on the radiative neutron-capture rates because, when the temperature is low, the (n, γ) and beta-decay rates (in the so-called "cold r-process") determine the final abundances. In the fission recycling model adopted here, the r-process path terminates in a region where beta-induced fission is much faster than the neutron-induced fission so that the r-process is always terminated by beta-induced fission. We note, however, that this depends upon the treatment of fission barriers and a different treatment (e.g. Korobkin et al. 2012) can result in a different mode of fission termination.

Once the r-process path fissions, we utilize the fission fragment distributions given in Ohta et al. (2008) and also the nuclear masses from the KTUY model (Koura et al. 2005). The fission barriers are extracted from the same KTUY model. However, since the KTUY model treats only the symmetric fission, we adopted here the two-center shell model to allow more general fission fragment distributions. The KTUY model has been shown within the GT2 theory to reproduce recent measurements of beta-decay half-lives of exotic neutron-rich isotopes (Nishimura et al. 2011). In a separate forthcoming study we will summarize a detailed comparison of the predictions of this model with known FFDs.

I also note that there have been numerous studies (e.g. Otsuki et al. 2003; Pfeiffer et al. 2001) of the sensitivity of this type of paradigm on various nuclear physics parameters. However, almost all MHDJ (or NDW) models (without shell quenching) show the abundance deficiencies on either side of the closed r-process abundance peaks. Moreover, the NDW and MHDJ supernova models often involve little or no fission recycling. As such, they do not depend on the details of fission rates and fragment distributions.

I note, however, that our NSM calculation (as shown below in Fig. 3.2) produces a different abundance pattern than that of previous NSM studies (Goriely et al. 2011; Korobkin et al. 2012; Goriely et al. 2013), especially in the region spanning between the 2nd and 3rd r-process peaks. There are two reasons for this difference: 1) The fission fragment distributions (FFDs); and 2) the number of fissioning nuclei contributing to fission recycling and the freezeout of the r-process distribution.

Regarding the FFDs, it has often been noted (e.g. Goriely et al. 2011; Korobkin et al. 2012; Goriely et al. 2013) that the elemental abundances from NSM calculations depend strongly on the FFD model. Admittedly this is a major uncertainty in all calculations of fission recycling in the r-process. As noted above, our FFD model is based upon the KTUY model plus a two-center shell model to predict both symmetric and asymmetric FFDs with up to three components. As such, fissile nuclei in our approach can span a wide mass range (A=100-180) of fission fragments. This is illustrated in the upper panel of Fig. 3.2 that shows the final abundance distribution compared with the FFDs of three illustrative nuclei.

On the other hand, the models of Korobkin et al. (2012) are mostly based upon a simple two fragment distribution as in Panov et al. (2001) (or alternatively the prescription of Kodama & Takahashi 1975). The assumption of only two fission daughter nuclei tends to place a large yield near the second r-process peak leading to a distribution that looks rather more like the solar r-process abundances. In contrast, the FFDs of Goriely et al. (2013) are based upon a rather sophisticated SPY revision (Panebianco et al. 2012) of the Wilkinson fission model (Wilkins et al. 1976). The main ingredient of this model is that the individual potential of each fission fragment is obtained as a function of its axial deformation from tabulated values. Then a Fermi gas state density is used to determine the main fission distribution. This leads to a multiple hump FFD similar to that considered here, but even with up to four humps. Although this arguably represents a more fundamental approach than that employed in the present work, we prefer the phenomenological FFD approach here as an alternative means to estimate fission yields far from stability.

An even more important difference between the present work and that of previous studies is the termination of the r-process path and the number of fissioning nuclei that contribute to fission recycling and the freezeout of the r-process abundances. The r-process path in our NSM calculations proceeds rather below the fissile region until nuclei with $A \sim 320$, whereas the r-process path in Goriely et al. (2013) terminates at $A \approx 278$ (or for a maximum $\langle Z \rangle$ for Korobkin

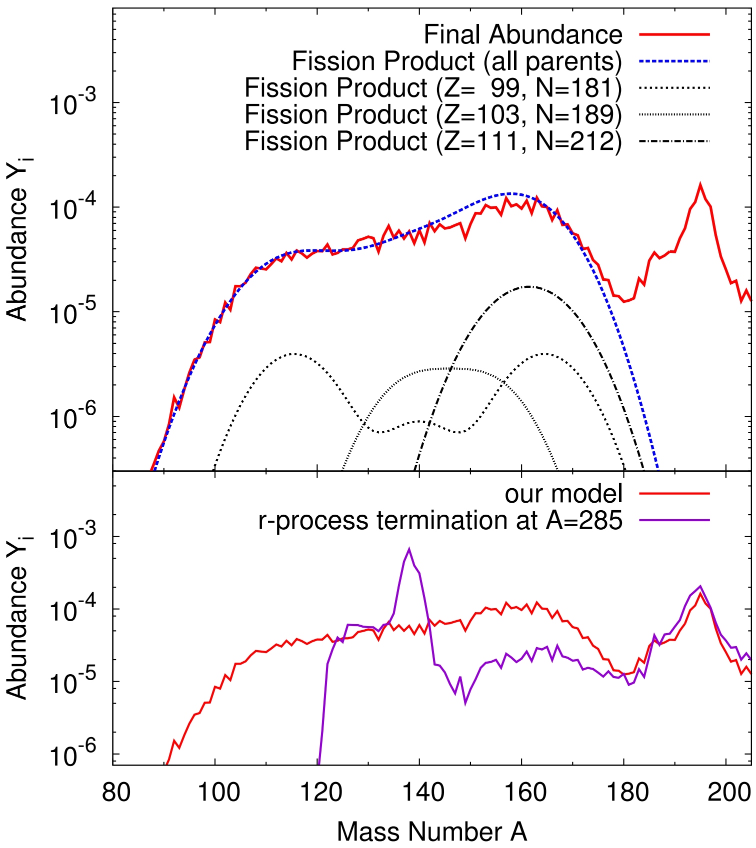

Figure 3.2: (Color online) Illustration of the impact of fission yields and fission recycling on the final r-process abundances. Upper panel shows the relative contributions for 3 representative nuclei compared with the final abundance distribution. The lower panel shows the same final r-process yields compared with the distribution that would result if fission recycling were only to occur from parent nuclei at the termination of the r-process path at $A = 285$.

et al. 2012). Moreover, we find that only $\sim 10\%$ of the final yield comes from the termination of the r-process path at N = 212 and Z = 111, while almost 90% of the $A = 160$ bump shown in Fig. 3.2 comes from the fission of more than 200 different parent nuclei mostly via beta-delayed fission. This is in contrast to the yields of Goriely et al. (2013) that are almost entirely due to a few $A \approx 278$ fissioning nuclei with a characteristic four hump FFD. This is the reason why they obtain a solar-like r-process like distribution.

To illustrate this point, in the lower panel of Fig. 3.2 we compare the yields of our model with a calculation in which we assume that the r-process path is terminated by symmetric fission of nuclei with $A = 285$. Clearly, in this case a solar-like distribution is obtained similar to that of Goriely et al. (2011), Korobkin et al. (2012) and Goriely et al. (2013). This highlights the importance of detailed fission probabilities along the r-process path.

Finally, we note that the apparent suppression of the the 3rd r-process peak in our final abundances relative to that of other works is caused by the large increase in the rare earth elements resulting from the FFDs of repeated fission recycling.

3.4 Relative r-Process Contributions

Figure 3.3 shows the main result of this study. The red line on Figure 3.3 shows the result of our fission recycling nucleosynthesis simulation summed over all trajectories of material ejected from the binary NSM model adopted here. This is compared with the abundances in the ejecta from the main r-process (blue line) from the MHDJ model of Nishimura et al. (2012), and also the NDW weak r-process abundances (green line) produced in the NDW from the 1.8 $M_\odot$ supernova core model of Wanajo (2013).

The key point of this figure is the important role that each process plays in producing the total abundance pattern of solar-system r-process abundances (black filled circles with error bars; Goriely 1999). The total abundance curve from all processes is shown as the black line on Figure 3.3. The weighting factor $f_{Fission}$ was determined from a normalization to isotopes near A=145-155 for the fission recycling (NSM) model. The factor f_{Weak} was determined from a fit to light isotopes near A=100 for the NDW model. The MHDJ yields were normalized to the second r-process peak. The best fit (black) line in Figure 3.3 is for $f_{Fission} = 0.16$ and $f_{Weak} = 4.3$, or roughly 79% weak, vs. 18% main, and $\sim$ 3% fission-recycling contributions with some uncertainty in the different models as noted above. Nevertheless, these estimated relative contributions are at least consistent with roughly estimated Galactic yields as described below.

Of particular relevance to the present study is that the underproduction of nuclides above and below the $A = 130$ r-process peak shown by the blue line is nearly accounted for by the fission recycling (NSM) and weak r-process (NDW) models. The final NSM r-process isotopic abundances from our adopted model for fission yields exhibit a very flat pattern due to several episodes of fission cycling. Thus, we find that fission recycling has the potential to resolve most of the underproduction problems for the elements just below and above the abundance peaks in models of the main r-process. The remaining underproduction below the $A = 130$ peak is most likely due to the weak r-process as illustrated on Figure 3.3.

The main point of this study is that one can deduce the relative contributions of each r-process model based upon their relative shortcomings. However, it is important to ask whether the inferred fractions, of ∼79% NDW, ∼18% MHDJ, and ∼3% NSM are plausible.

Although there are many uncertainties in the astrophysical and galactic chemical evolution parameters (Argast et al. 2000; Komiya et al. 2014), it is worthwhile to estimate weight parameters $f_{Fission}$ and f_{Weak} from observed Galactic event rates and expected yields. In particular we write

$$f_{Fission} \approx \frac{\mathrm{R_{NSM} M_{r,NSM}}}{\epsilon_{MHDJ} \mathrm{R_{CCSN} M_{r,MHDJ}}} \quad , \tag{3.6}$$

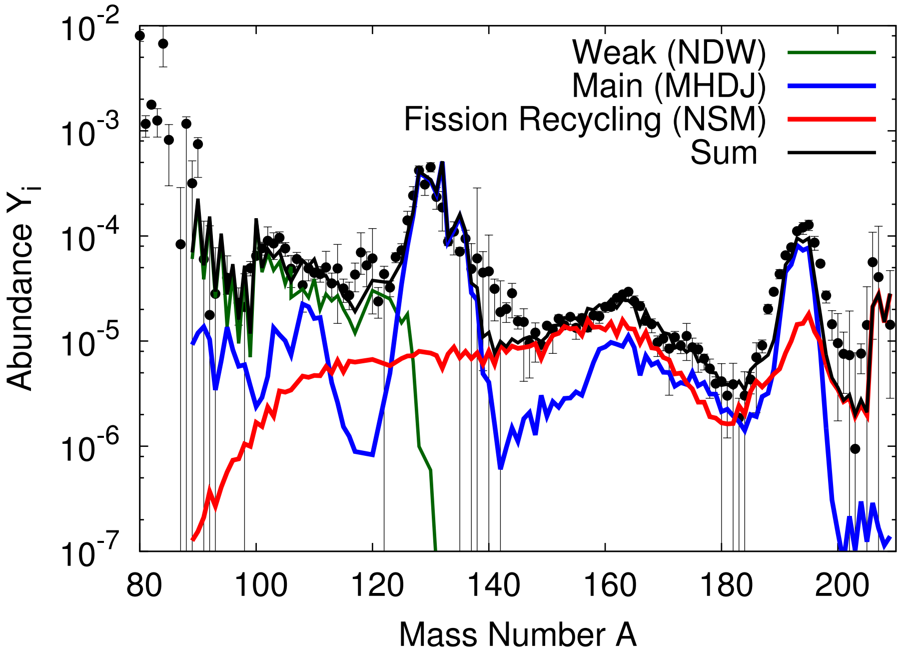

Figure 3.3: (Color online) Average final abundance patterns for the fission recycling environment of NSM (red line), the main r-process abundances from the MHDJ model (blue line) and weak r-process (green line) from the NDW. These are compared with the observed (Goriely 1999) r-process abundances in the solar system (black dots). The thin black line shows the sum of all contributions.

and

$$f_{Weak} \approx \frac{\mathrm{R_{CCSN}M_{r,Weak}}}{\epsilon_{MHDJ}\mathrm{R_{CCSN}M_{r,MHDJ}}} \quad , \tag{3.7}$$

where $\mathrm{M_{r,NSM}}$, $\mathrm{M_{r,MHDJ}}$, and $\mathrm{M_{r,Weak}}$ are the ejected masses of r-elements from the NSM, MHDJ, and NDW r-process models, respectively, while $\mathrm{R_{CCSN}}$ and $\mathrm{R_{NSM}}$ are the corresponding relative Galactic event rates of CCSNe and NSMs.

The ejected mass of r-process elements in the models of Wanajo (2013) is $\approx 2 \times 10^{-5}$ $\mathrm{M_\odot}$ and nearly independent of assumed core mass. The quantity ϵ_{MHDJ} is the fraction of CCSNe that result in magneto-rotationally driven jets. This was estimated in Winteler et al. (2012) to be $\sim 1\%$ of the core-collapse supernova rate based upon the models of Woosley & Heger (2006). However this is probably uncertain by at least a factor of two. Indeed, the fraction could be larger as most massive stars are fast rotators and the conservation of magnetic flux should often lead to high magnetic fields in the newly formed proto-neutron star. Hence, this fraction could easily range from ~ 1 to $\sim 5\%$ which incorporates the $\sim 1\%$ fraction of observed magnetars compared to normal neutron stars. (We treat this as a lower limit because some fraction of observed normal neutron stars may have had a larger magnetic field in the past.) The mass of synthesized r-process elements from MHDJs is estimated to be $6{\times}10^{-3}M_\odot$ (Winteler et al. 2012) while that of a typical binary NSM is expected to be $2 \pm 1 \times 10^{-2}M_\odot$ (Korobkin et al. 2012). If the Galactic neutron star merger rate is 80^{+200}_{-70} $\mathrm{Myr^{-1}}$ (Kalogera et al. 2004), and the Galactic supernova rate is $1.9 \pm 1.1 \times 10^4$ $\mathrm{Myr^{-1}}$ (Diehl et al. 2006), then one should expect $f_{Fission} \sim 0.6 \pm 0.4$ and $f_{Weak} \approx 8 \pm 6$ corresponding to relative contributions of $\sim 80\%$ weak, $\sim 10\%$ main and ~ 10 % fission recycling. Thus, although there are large uncertainties, these fractions are plausibly consistent with our fit parameters. This suggests that such a fit may be a way of constraining the relative contribution of NSMs and CCSNe to solar-system material.

We note, however, that other NSM calculations predict about 10^{-4} to 10^{-2} $\mathrm{M_\odot}$ of r-process material to be ejected (e.g. Hotokezaka et al. 2013; Bauswein et al. 2013). Adopting a value of 10^{-3} $\mathrm{M_\odot}$ could lead to $f_{Fission} \sim 0.02$, i.e. about an order of magnitude below that suggested in our fit to Figure 3.3.

Of course, this needs to be better quantified in more detailed chemical evolution (Cescutti & Chiappini 2014; Cescutti et al. 2015; Tsujimoto & Shigeyama 2014a,b; Komiya et al. 2014; Ishimaru et al. 2015; Wehmeyer et al. 2015) and chemodynamical studies (Shen et al. 2015; van de Voort et al. 2015) along with better r-process hydrodynamic models (Winteler et al. 2012; Perego et al. 2014; Rosswog et al. 2014; Wanajo et al. 2014; Goriely et al. 2015; Just et al. 2015; Nishimura et al. 2015). Nevertheless, based upon the models adopted here, the inferred division of r-process contributions remains at least plausible.

3.5 Universality of r-Process Elemental Abundances

In the above we have not discussed a very important clue to the origin of r-process abundances. It is by now well established (Sneden et al. 2008) that the elemental abundances in many metal-poor stars show a pattern that is very similar to that of the solar-system r-process distribution, particularly in the range of $55 < Z < 70$. This however, can pose a difficulty (Mathews et al. 1992; Argast et al. 2000) for NSM models (either in the present work or in other studies). That is because metal-poor stars are thought to have arrived very early in the history of the Galaxy, whereas NSMs require a relatively long gravitational radiation orbit decay time prior to merger (~ 0.1 Gyr). Whatever the situation, it is of value to examine the impact of the possible late arrival of fission recycling material on the r-process elemental abundance distribution in metal-poor stars.

Figure 3.4 shows the elemental abundance distribution calculated in two scenarios, i.e. with and without the fission recycling yields of NSMs. These are compared with the observed elemental r-process abundances in two well-studied metal-poor r-process enhanced stars, HD1601617 (Roederer & Lawler 2012) and CS22892-052 (Sneden et al. 2003). Here, we note that there is little distinction between the two curves (although the fit is slightly better when the fission recycling yields are included). The reason for this insensitivity is that the fission recycling environment only contributes about 3% to the total r-process abundance. Although this yield is important to fill in the isotopic abundances above and below the r-process peaks, and also to make the rare-earth bump near A=160, there is little apparent difference in the elemental abundances with or without neutron star mergers. Among other things, this is because the region below the peak ($Z \sim 50$) is poorly sampled, and moreover, summing over isotopes to produce elemental averages somewhat washes out the underproduction above and below the r-process mass peaks. Hence, the elemental r-process abundances in metal poor stars do not clearly require that fission recycling occurred early in the Galaxy.

We do note, however that the dispersion in the stars themselves for the lightest elements ($30 < Z < 50$) is suggestive that not all CCSNe contribute both a weak and main r-process. This is consistent with the expectation that the NDW could occur in all CCSNe while the main r-process from the MHDJ will only occur in a limited fraction of CCSNe, i.e. those with rotation and strong magnetic fields.

3.6 Discussion

The fits to the abundance distribution (e.g. Figure 3.3) are as good as or better than most models in the literature. Nevertheless, it is worthwhile, to address some of the detailed deficiencies in

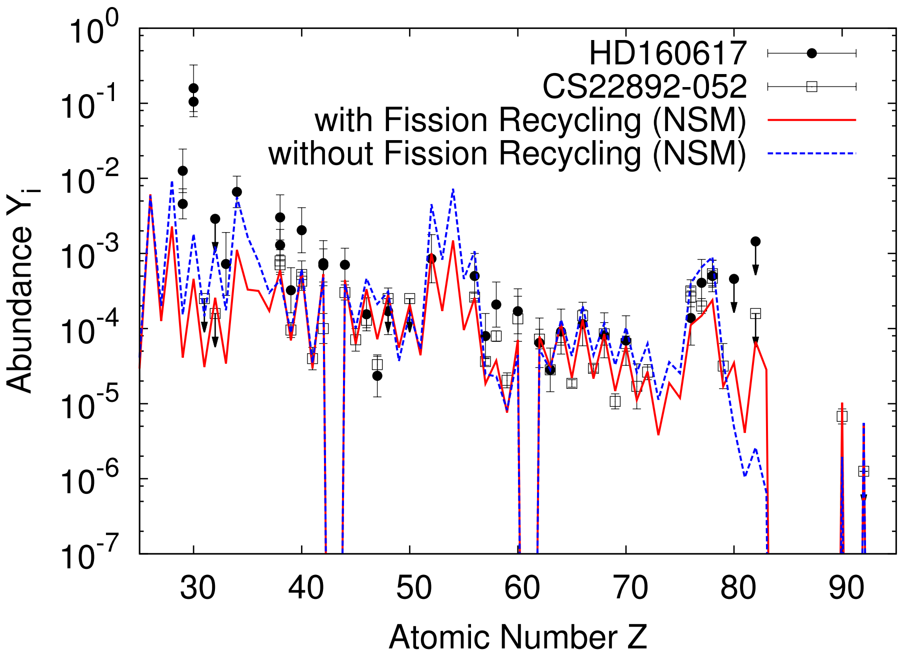

Figure 3.4: (Color online) Average final elemental abundances for the total sum from Fig. 3.2 (solid line) and the contribution without NSMs (dashed line). These are compared with the observed elemental r-process abundances in two well-studied metal-poor r-process enhanced stars, HD1601617 (filled circles; Roederer & Lawler 2012) and CS22892-052 (open squares; Sneden et al. 2003). The curves are arbitrarily normalized at europium (Z=63).

both Figures 3.2 and 3.3. For example, although the r-process peaks at A=130 and 195 along with the rare-earth peak region A = 145-180 in Figure 3.3 are remarkably well reproduced, there are some differences just above the main r-process peaks in the regions of A=140-145 and 200-205. We note, however, that these isotopes have the largest uncertainties in the r-process abundances themselves as is visible on Figure 3.3. Hence, these discrepancies may simply reflect the abundance uncertainties, although the possibility remains of a shortcoming in the models for these isotopes.

Similarly, in Figure 3.4 there is an underproduction of elements at Z=58 and 60. The abundance of Ce (Z=58) in Figure 4 is well determined observationally for CS22892-052 as follows: $\log \epsilon(\mathrm{Ce}) = -0.50 \pm 0.07$ (Sneden et al. 2003) and $= -0.38 \pm 0.08$ (Honda et al. 2004). This corresponds to the deficient isotopes with A=140 and 142 in Figure 3.3. However, the odd elements with Z= 57 (La) and Z=59 (Pr) are reproduced. This suggests that the odd-even effect in the region of lanthanide elements may be underestimated in the mass model employed here. Nevertheless, the main point of this study is not to give a precise reproduction of r-process elemental abundances but rather to demonstrate the possibility that fission recycling supplements the underproduced elements. Clearly, a better understanding of the nuclear uncertainties within this context is still needed.

We also note that there is a possible deficiency of Pb (Z=82) in Figure 3.4. This, however, may relate to observational uncertainties. There are two measured Pb abundances for CS22892-052 in Sneden et al. (2003). One was a ground-based measurement, while the other was obtained with *HST*. However, both of these values should be considered upper limits. In Sneden et al. (2003) it was noted that the suggested detections of the two Pb I lines in the ground-based spectra should be nearly 10 times weaker than the $\lambda = 2833.05$ line, that could not be detected in the HST spectrum. Hence, the derived Pb abundance upper limit from the $\lambda = 2833$ line is probably more reliable than the abundances determined from the questionable detections of the other two Pb I lines. Thus, one should abandon the Pb abundance of $\log \epsilon(\mathrm{Pb}) = 0.05$ from the ground-based observation in favor of $\log \epsilon(\mathrm{Pb}) < -0.2$ from the HST observation. We also note that the more recent observation of Roederer et al. (2009) also obtains $\log \epsilon(\mathrm{Pb}) < -0.15$. These upper limits are consistent with our calculation.

Another issue worthy of discussion is that of Th (Z=90) and U (Z=92) production in Figure 3.4. Th has been observed in a number of metal-poor stars and U in a few. This indicates that the r-process mechanism at work in the early Galaxy could produce the actinide elements and beyond. Although one tends to think that the production of actinide elements requires a fission-recycling r-process, in fact the production of Th and U is possible even in models that do not lead to fission recycling. For example, the MHDJ models with strong magnetic fields in Nishimura et al. (2015) could produce Th and U in as much as their solar abundances. On the other hand, MHDJ models with weak magnetic fields tend to produce actinides below solar abundances. Hence, the observation of Th and U in metal-poor stars constrains the early astrophysical environment, but does not necessarily require that a fission-recycling r-process (such as the NSM model) contributed to metal-poor stars.

3.7 Conclusions

In summary, we have considered the relative contributions of three generic r-process environments to the solar-system r-process abundances and the abundances in r-process enhanced metal-poor stars. These environments are discussed in the context of neutron star mergers, neutrino driven winds and magnetohydrodynamically driven jets, although these environments should be considered as illustrative and not definitive of the specific r-process environments. Nevertheless, based upon our adopted fission fragment distributions we find that the relative contributions from each environment has the possibility of explaining a unique feature of the r-process abundances. Moreover, the deduced relative contributions are plausibly consistent with galactic chemical evolution considerations.

Clearly, more work along this line is required to explain details. Nevertheless, we suggest that the possibility that all three general environments occur in detectable amounts in the r-process distribution should be taken seriously in future investigations of the origin of r-process nuclides.

Chapter 4

Protomagnetar Wind Simulation in 1.5D GRMHD Framework and r-Process Nucleosynthesis

本章については、5 年以内に雑誌等で刊行予定のため、非公開。

Chapter 5

Summary of This Thesis

Astrophysical origin of heavy elements is one of the biggest problems in science. The r-process is responsible for production of half of heavy elements beyond iron. Since Burbidge et al. (1957), the attempts to investigate where the r-process occurs have been done. Multiple astrophysical events such as neutrino-driven winds in core-collapse supernovae, magnetohydrodynamic (MHD) jet supernovae and binary neutron star mergers have been proposed as sources of r-process elements. But the r-process origin remains unclear. One of the main reasons is ambiguity of theoretical nuclear and astrophysical modeling. Full theoretical calculations require much larger computational costs than currently available. So we need to take some simplifications for modeling, which causes some uncertainties.

In this thesis, we investigated two questions involved with magneto-rotational supernovae: 1. how the underproduction problem of the r-process in MHD jet supernovae is solved, 2. what elements are synthesized in protomagnetar winds of magneto-rotational supernovae.

In the first study, we comprehensively discussed a possibility that the multiple r-process sites, i.e. neutrino-driven winds in core-collapse supernovae, MHD jet supernovae and binary neutron star mergers, are supplemented each other to form the solar r-process abundances. We carried out r-process simulations of binary neutron star mergers with a realistic fission model. We found that our fission model predicts that neutron-rich fissile nuclei are distributed in a heavier region than previous models. This feature results in production of the large number of fission yields, in piling up nuclear abundances on both sides of the 2nd r-process peak and in formation of the very flat abundance pattern in a range of $A \sim 100 - 160$. This unique abundance pattern allows us to supplement the underproduction of MHD jet supernovae and we estimated 3% contribution of neutron star mergers to the solar system r-process abundances. We also found that comparison between their theoretical r-process calculations and the elemental r-process abundances in metal poor stars does not clearly require that neutron star mergers occurred early in the Galaxy. From this result, we proposed a scenario that neutrino-driven winds and MHD jet supernovae supply r-process elements in the early galaxies, and later neutron star mergers start to release r-elements.

In the second study, 本研究については、5年以内に雑誌等で刊行予定のため、非公開。

To reach a definitive conclusion, more sophisticated nuclear and astrophysical models are clearly desirable. Such efforts will finally judge the scenario proposed above and quantitative correctness of simplifications assumed in many theoretical studies.

Acknowledgements

I am grateful to my supervisor, Professor Toshitaka Kajino, for his contribution to my research and my research life. I was helped by his notices and wide knowledge many times. His both microscopic and macroscopic view points made my study rich and I learned an approach to scientific problems through discussions with him. Thanks to his cooperation, I got experiences to visit foreign countries collaborate with international scientists. I am happy to get such precious experiences. I really enjoyed my research life over last five years.

I am indebted to Tomoya Takiwaki for his continuous and patient support. I have learned lots of knowledge on the supernova physics and numerical simulations of fluid dynamics from him. I could not complete the supernova study without his cooperation.

I also thank all my collaborators, Grant J. Mathews, Satoshi Chiba, Shunji Nishimura and Giuseppe Lorusso for their deep insights and valuable discussions.

Bibliography

Akiyama, S., Wheeler, J. C., Meier, D. L., & Lichtenstadt, I., "The Magnetorotational Instability in Core-Collapse Supernova Explosions", *Astrophysical Journal*, **584**, 954, (2003).

Arcones, A., & Martínez-Pinedo, G., "Dynamical r-process studies within the neutrino-driven wind scenario and its sensitivity to the nuclear physics input", *Physical Review C*, **83**, 045809, (2011).

Argast, D., Samland, M., Gerhard, O. E., & Thielemann, F.-K., "Metal-poor halo stars as tracers of ISM mixing processes during halo formation", *Astronomy and Astrophysics*, **356**, 873, (2000).

Arnould, M., Goriely, S., & Takahashi, K., "The r-process of stellar nucleosynthesis: Astrophysics and nuclear physics achievements and mysteries", *Phys. Rep.*, **450**, 97, (2007).

Bauswein, A., Goriely, S., & Janka, H.-T., "Systematics of Dynamical Mass Ejection, Nucleosynthesis, and Radioactively Powered Electromagnetic Signals from Neutron-star Mergers", *Astrophysical Journal*, **773**, 78, (2013).

Bruenn, S. W., "Stellar core collapse - Numerical model and infall epoch", *Astrophysical Journal Supplement*, **58**, 771, (1985).

Burbidge, E. M., Burbidge, G. R., Fowler, W. A., & Hoyle, F., "Synthesis of the Elements in Stars", *Reviews of Modern Physics*, **29**, 547, (1957).

Burrows, A., Dessart, L., Livne, E., Ott, C. D., & Murphy, J., "Simulations of Magnetically Driven Supernova and Hypernova Explosions in the Context of Rapid Rotation", *Astrophysical Journal*, **664**, 416, (2007).

Cerdá-Durán, P., Font, J. A., Antón, L., & Müller, E., "A new general relativistic magnetohydrodynamics code for dynamical spacetimes", *Astronomy and Astrophysics*, **492**, 937, (2008).

Cescutti, G., & Chiappini, C., "Explaining the Ba, Y, Sr, and Eu abundance scatter in metal-poor halo stars: constraints to the r-process", *Astronomy and Astrophysics*, **565**, A51, (2014).

Cescutti, G., Romano, D., Matteucci, F., Chiappini, C., & Hirschi, R., "The role of neutron star mergers in the chemical evolution of the Galactic halo", *Astronomy and Astrophysics*, **577**, A139, (2015).

Chiba, S., Koura, H., Maruyama, T., et al., "The r-process element abundance with a realistic fission fragment mass distribution", in *American Institute of Physics Conference Series*, Vol. 1016, *Origin of Matter and Evolution of Galaxies*, ed. T. Suda, T. Nozawa, A. Ohnishi, K. Kato, M. Y. Fujimoto, T. Kajino, & S. Kubono, 162–167, (2008).

Diehl, R., Halloin, H., Kretschmer, K., et al., "Radioactive ^{26}Al from massive stars in the Galaxy", *Nature*, **439**, 45, (2006).

Eichler, D., Livio, M., Piran, T., & Schramm, D. N., "Nucleosynthesis, neutrino bursts and gamma-rays from coalescing neutron stars", *Nature*, **340**, 126, (1989).

Eichler, M., Arcones, A., Kelic, A., et al., "The Role of Fission in Neutron Star Mergers and Its Impact on the r-Process Peaks", *Astrophysical Journal*, **808**, 30, (2015).

Erler, J., Langanke, K., Loens, H. P., Martínez-Pinedo, G., & Reinhard, P.-G., "Fission properties for r-process nuclei", *Physical Review C*, **85**, 025802, (2012).

Etienne, Z. B., Liu, Y. T., Paschalidis, V., & Shapiro, S. L., "General relativistic simulations of black-hole-neutron-star mergers: Effects of magnetic fields", *Physical Review D*, **85**, 064029, (2012).

Farouqi, K., Kratz, K.-L., Pfeiffer, B., et al., "Charged-particle and Neutron-capture Processes in the High-entropy Wind of Core-collapse Supernovae", *Astrophysical Journal*, **712**, 1359, (2010).

Fischer, T., Whitehouse, S. C., Mezzacappa, A., Thielemann, F.-K., & Liebendörfer, M., "Protoneutron star evolution and the neutrino-driven wind in general relativistic neutrino radiation hydrodynamics simulations", *Astronomy and Astrophysics*, **517**, A80, (2010).

Freiburghaus, C., Rembges, J.-F., Rauscher, T., et al., "The Astrophysical r-Process: A Comparison of Calculations following Adiabatic Expansion with Classical Calculations Based on Neutron Densities and Temperatures", *Astrophysical Journal*, **516**, 381, (1999).

Fujimoto, S.-i., Hashimoto, M.-a., Kotake, K., & Yamada, S., "Heavy-Element Nucleosynthesis in a Collapsar", *Astrophysical Journal*, **656**, 382, (2007).

Fujimoto, S.-i., Nishimura, N., & Hashimoto, M.-a., "Nucleosynthesis in Magnetically Driven Jets from Collapsars", *Astrophysical Journal*, **680**, 1350, (2008).

Goriely, S., "Uncertainties in the solar system r-abundance distribution", *Astronomy and Astrophysics*, **342**, 881, (1999).

Goriely, S., Bauswein, A., & Janka, H.-T., "r-process Nucleosynthesis in Dynamically Ejected Matter of Neutron Star Mergers", *Astrophysical Journal Letters*, **738**, L32, (2011).

Goriely, S., Bauswein, A., Just, O., Pllumbi, E., & Janka, H.-T., "Impact of weak interactions of free nucleons on the r-process in dynamical ejecta from neutron star mergers", *Monthly Notices of the Royal Astronomical Society*, **452**, 3894, (2015).

Goriely, S., Sida, J.-L., Lemaître, J.-F., et al., "New Fission Fragment Distributions and r-Process Origin of the Rare-Earth Elements", *Physical Review Letters*, **111**, 242502, (2013).

Heger, A., Langer, N., & Woosley, S. E., "Presupernova Evolution of Rotating Massive Stars. I. Numerical Method and Evolution of the Internal Stellar Structure", *Astrophysical Journal*, **528**, 368, (2000).

Honda, S., Aoki, W., Kajino, T., et al., "Spectroscopic Studies of Extremely Metal-Poor Stars with the Subaru High Dispersion Spectrograph. II. The r-Process Elements, Including Thorium", *Astrophysical Journal*, **607**, 474, (2004).

Hotokezaka, K., Kiuchi, K., Kyutoku, K., et al., "Mass ejection from the merger of binary neutron stars", *Physical Review D*, **87**, 024001, (2013).

Hüdepohl, L., Müller, B., Janka, H.-T., Marek, A., & Raffelt, G. G., "Neutrino Signal of Electron-Capture Supernovae from Core Collapse to Cooling", *Physical Review Letters*, **104**, 251101, (2010).

Ishimaru, Y., Wanajo, S., & Prantzos, N., "Neutron Star Mergers as the Origin of r-process Elements in the Galactic Halo Based on the Sub-halo Clustering Scenario", *Astrophysical Journal Letters*, **804**, L35, (2015).

Iwamoto, A., Yamaji, S., Suekane, S., & Harada, K., "Potential Energy Surfaces for the Fission of the Actinide Nuclei", *Progress of Theoretical Physics*, **55**, 115, (1976).

Jin, Z.-P., Li, X., Cano, Z., et al., "The Light Curve of the Macronova Associated with the Long-Short Burst GRB 060614", *Astrophysical Journal Letters*, **811**, L22, (2015).

Just, O., Bauswein, A., Pulpillo, R. A., Goriely, S., & Janka, H.-T., "Comprehensive nucleosynthesis analysis for ejecta of compact binary mergers", *Monthly Notices of the Royal Astronomical Society*, **448**, 541, (2015).

Kalogera, V., Kim, C., Lorimer, D. R., et al., "The Cosmic Coalescence Rates for Double Neutron Star Binaries", *Astrophysical Journal Letters*, **601**, L179, (2004), erratum-ibid. 614:L137L138, October 2004.

Kasen, D., Badnell, N. R., & Barnes, J., "Opacities and Spectra of the r-process Ejecta from Neutron Star Mergers", *Astrophysical Journal*, **774**, 25, (2013).

Kodama, T., & Takahashi, K., "R-process nucleosynthesis and nuclei far from the region of β-stability", *Nuclear Physics A*, **239**, 489, (1975).

Komiya, Y., Yamada, S., Suda, T., & Fujimoto, M. Y., "The New Model of Chemical Evolution of r-process Elements Based on the Hierarchical Galaxy Formation. I. Ba and Eu", *Astrophysical Journal*, **783**, 132, (2014).

Korobkin, O., Rosswog, S., Arcones, A., & Winteler, C., "On the astrophysical robustness of the neutron star merger r-process", *Monthly Notices of the Royal Astronomical Society*, **426**, 1940, (2012).

Koura, H., "Ground-state properties of heavy and superheavy nuclei predicted by nuclear mass models", in *American Institute of Physics Conference Series*, Vol. 704, *Tours Symposium on Nuclear Physics V*, ed. M. Arnould, M. Lewitowicz, G. Münzenberg, H. Akimune, M. Ohta, H. Utsunomiya, T. Wada, & T. Yamagata, 60–72, (2004).

Koura, H., Tachibana, T., Uno, M., & Yamada, M., "Nuclidic Mass Formula on a Spherical Basis with an Improved Even-Odd Term", *Progress of Theoretical Physics*, **113**, 305, (2005).

Kratz, K.-L., Farouqi, K., & Möller, P., "A High-entropy-wind r-process Study Based on Nuclear-structure Quantities from the New Finite-range Droplet Model Frdm(2012)", *Astrophysical Journal*, **792**, 6, (2014).

Kulkarni, S. R., "Modeling Supernova-like Explosions Associated with Gamma-ray Bursts with Short Durations", *ArXiv Astrophysics e-prints*, astro-ph/0510256, (2005).

Lattimer, J. M., & Schramm, D. N., "Black-hole-neutron-star collisions", *Astrophysical Journal Letters*, **192**, L145, (1974).

—, "The tidal disruption of neutron stars by black holes in close binaries", *Astrophysical Journal*, **210**, 549, (1976).

LeBlanc, J. M., & Wilson, J. R., "A Numerical Example of the Collapse of a Rotating Magnetized Star", *Astrophysical Journal*, **161**, 541, (1970).

Li, L.-X., & Paczyński, B., "Transient Events from Neutron Star Mergers", *Astrophysical Journal Letters*, **507**, L59, (1998).

Lodders, K., "Solar System Abundances of the Elements", *Astrophysics and Space Science Proceedings*, **16**, 379, (2010).

Lorusso, G., Nishimura, S., Xu, Z. Y., et al., "β -Decay Half-Lives of 110 Neutron-Rich Nuclei across the N =82 Shell Gap: Implications for the Mechanism and Universality of the Astrophysical r Process", *Physical Review Letters*, **114**, 192501, (2015).

Martínez-Pinedo, G., Mocelj, D., Zinner, N. T., et al., "The role of fission in the r-process", *Progress in Particle and Nuclear Physics*, **59**, 199, (2007).

Mathews, G. J., Bazan, G., & Cowan, J. J., "Evolution of heavy-element abundances as a constraint on sites for neutron-capture nucleosynthesis", *Astrophysical Journal*, **391**, 719, (1992).

Mathews, G. J., & Ward, R. A., "Neutron capture processes in astrophysics", *Reports on Progress in Physics*, **48**, 1371, (1985).

Metzger, B. D., Thompson, T. A., & Quataert, E., "Proto-Neutron Star Winds with Magnetic Fields and Rotation", *Astrophysical Journal*, **659**, 561, (2007).

Metzger, B. D., Martínez-Pinedo, G., Darbha, S., et al., "Electromagnetic counterparts of compact object mergers powered by the radioactive decay of r-process nuclei", *Monthly Notices of the Royal Astronomical Society*, **406**, 2650, (2010).

Meyer, B. S., & Brown, J. S., "Survey of r-Process Models", *Astrophysical Journal Supplement*, **112**, 199, (1997).

Möller, P., Myers, W. D., Sagawa, H., & Yoshida, S., "New Finite-Range Droplet Mass Model and Equation-of-State Parameters", *Physical Review Letters*, **108**, 052501, (2012).

Möller, P., Nix, J. R., Myers, W. D., & Swiatecki, W. J., "Nuclear Ground-State Masses and Deformations", *Atomic Data and Nuclear Data Tables*, **59**, 185, (1995).

Mösta, P., Richers, S., Ott, C. D., et al., "Magnetorotational Core-collapse Supernovae in Three Dimensions", *Astrophysical Journal Letters*, **785**, L29, (2014a).

Mösta, P., Mundim, B. C., Faber, J. A., et al., "GRHydro: a new open-source general-relativistic magnetohydrodynamics code for the Einstein toolkit", *Classical and Quantum Gravity*, **31**, 015005, (2014b).

Mumpower, M. R., Surman, R., McLaughlin, G. C., & Aprahamian, A., “The impact of individual nuclear properties on r-process nucleosynthesis”, *Progress in Particle and Nuclear Physics*, **86**, 86, (2016).

Myers, W. D., & ŚwiaŢecki, W. J., “Thomas-Fermi fission barriers”, *Physical Review C*, **60**, 014606, (1999).

Nagataki, S., & Kohri, K., “The r-Process Nucleosynthesis in Neutrino-/Magnetocentrifugally-Driven Winds”, *PASJ*, **53**, 547, (2001).

Nakamura, K., Kajino, T., Mathews, G. J., Sato, S., & Harikae, S., “a Review of r-PROCESS Nucleosynthesis in the Collapsar Jet”, *International Journal of Modern Physics E*, **22**, 1330022, (2013).

—, “r-process nucleosynthesis in the MHD+neutrino-heated collapsar jet”, *Astronomy and Astrophysics*, **582**, A34, (2015).

Nishimura, N., Kajino, T., Mathews, G. J., Nishimura, S., & Suzuki, T., “Impact of new β-decay half-lives on r-process nucleosynthesis”, *Physical Review C*, **85**, 048801, (2012).

Nishimura, N., Takiwaki, T., & Thielemann, F.-K., “The r-process Nucleosynthesis in the Various Jet-like Explosions of Magnetorotational Core-collapse Supernovae”, *Astrophysical Journal*, **810**, 109, (2015).

Nishimura, S., Kotake, K., Hashimoto, M.-a., et al., “r-Process Nucleosynthesis in Magnetohydrodynamic Jet Explosions of Core-Collapse Supernovae”, *Astrophysical Journal*, **642**, 410, (2006).

Nishimura, S., Li, Z., Watanabe, H., et al., “β-Decay Half-Lives of Very Neutron-Rich Kr to Tc Isotopes on the Boundary of the r-Process Path: An Indication of Fast r-Matter Flow”, *Physical Review Letters*, **106**, 052502, (2011).

Noble, S. C., Gammie, C. F., McKinney, J. C., & Del Zanna, L., “Primitive Variable Solvers for Conservative General Relativistic Magnetohydrodynamics”, *Astrophysical Journal*, **641**, 626, (2006).

O’Connor, E., & Ott, C. D., “A new open-source code for spherically symmetric stellar collapse to neutron stars and black holes”, *Classical and Quantum Gravity*, **27**, 114103, (2010).

Ohta, M., Tatsuda, S., Hashizume, T., et al., “Systematic study for the mass distribution of fission fragments in the neutron rich region”, in *Proceedings of International Conference on Nuclear Data for Science and Technology*, ed. O. Bersillon, F. Gunsing, E. Bauge, R. Jacqmin, & S. Leray (EDP Sciences), 359–362, (2008).

Ono, M., Hashimoto, M., Fujimoto, S., Kotake, K., & Yamada, S., "Explosive Nucleosynthesis in Magnetohydrodynamical Jets from Collapsars. II — Heavy-Element Nucleosynthesis of s, p, r-Processes", *Progress of Theoretical Physics*, **128**, 741, (2012).

Otsuki, K., Mathews, G. J., & Kajino, T., "r-Process abundance universality and actinide cosmochronology", *New Astronomy*, **8**, 767, (2003).

Panebianco, S., Sida, J.-L., Goutte, H., et al., "Role of deformed shell effects on the mass asymmetry in nuclear fission of mercury isotopes", *Physical Review C*, **86**, 064601, (2012).

Panov, I. V., Freiburghaus, C., & Thielemann, F.-K., "Could fission provide the formation of chemical elements with $A \leqq 120$ in metal-poor stars?", *Nuclear Physics A*, **688**, 587, (2001).

Perego, A., Rosswog, S., Cabezón, R. M., et al., "Neutrino-driven winds from neutron star merger remnants", *Monthly Notices of the Royal Astronomical Society*, **443**, 3134, (2014).

Pfeiffer, B., Kratz, K.-L., Thielemann, F.-K., & Walters, W. B., "Nuclear structure studies for the astrophysical r-process", *Nuclear Physics A*, **693**, 282, (2001).

Piran, T., Nakar, E., & Rosswog, S., "The electromagnetic signals of compact binary mergers", *Monthly Notices of the Royal Astronomical Society*, **430**, 2121, (2013).

Qian, Y.-Z., & Woosley, S. E., "Nucleosynthesis in Neutrino-driven Winds. I. The Physical Conditions", *Astrophysical Journal*, **471**, 331, (1996).

Radice, D., Galeazzi, F., Lippuner, J., et al., "Dynamical mass ejection from binary neutron star mergers", *Monthly Notices of the Royal Astronomical Society*, **460**, 3255, (2016).

Roederer, I. U., Kratz, K.-L., Frebel, A., et al., "The End of Nucleosynthesis: Production of Lead and Thorium in the Early Galaxy", *Astrophysical Journal*, **698**, 1963, (2009).

Roederer, I. U., & Lawler, J. E., "Detection of Elements at All Three r-process Peaks in the Metal-poor Star HD 160617", *Astrophysical Journal*, **750**, 76, (2012).

Romero, J. V., Ibanez, J. M. A., Marti, J. M. A., & Miralles, J. A., "A New Spherically Symmetric General Relativistic Hydrodynamical Code", *Astrophysical Journal*, **462**, 839, (1996).

Rosswog, S., "Astrophysical smooth particle hydrodynamics", *New Astronomy Reviews*, **53**, 78, (2009).

Rosswog, S., Korobkin, O., Arcones, A., Thielemann, F.-K., & Piran, T., "The long-term evolution of neutron star merger remnants - I. The impact of r-process nucleosynthesis", *Monthly Notices of the Royal Astronomical Society*, **439**, 744, (2014).

Rosswog, S., & Liebendörfer, M., "High-resolution calculations of merging neutron stars - II. Neutrino emission", *Monthly Notices of the Royal Astronomical Society*, **342**, 673, (2003).

Rosswog, S., Piran, T., & Nakar, E., "The multimessenger picture of compact object encounters: binary mergers versus dynamical collisions", *Monthly Notices of the Royal Astronomical Society*, **430**, 2585, (2013).

Ruffert, M., Janka, H.-T., & Schaefer, G., "Coalescing neutron stars - a step towards physical models. I. Hydrodynamic evolution and gravitational-wave emission.", *Astronomy and Astrophysics*, **311**, 532, (1996).

Sasaqui, T., Kajino, T., Mathews, G. J., Otsuki, K., & Nakamura, T., "Sensitivity of r-Process Nucleosynthesis to Light-Element Nuclear Reactions", *Astrophysical Journal*, **634**, 1173, (2005).

Sato, K., Yamaji, S., Harada, K., & Yoshida, S., "A numerical analysis of the heavy-ion reaction based on the linear response theory", *Zeitschrift fur Physik A Hadrons and Nuclei*, **290**, 149, (1979).

Sawai, H., & Yamada, S., "Influence of Magnetorotational Instability on Neutrino Heating: A New Mechanism for Weakly Magnetized Core-collapse Supernovae", *Astrophysical Journal Letters*, **784**, L10, (2014).

Sawai, H., Yamada, S., & Suzuki, H., "Global Simulations of Magnetorotational Instability in the Collapsed Core of a Massive Star", *Astrophysical Journal Letters*, **770**, L19, (2013).

Shen, H., Toki, H., Oyamatsu, K., & Sumiyoshi, K., "Relativistic equation of state of nuclear matter for supernova and neutron star", *Nuclear Physics A*, **637**, 435, (1998a).

—, "Relativistic Equation of State of Nuclear Matter for Supernova Explosion", *Progress of Theoretical Physics*, **100**, 1013, (1998b).

Shen, S., Cooke, R. J., Ramirez-Ruiz, E., et al., "The History of R-Process Enrichment in the Milky Way", *Astrophysical Journal*, **807**, 115, (2015).

Shibata, M., Liu, Y. T., Shapiro, S. L., & Stephens, B. C., "Magnetorotational collapse of massive stellar cores to neutron stars: Simulations in full general relativity", *Physical Review D*, **74**, 104026, (2006).

Sneden, C., Cowan, J. J., & Gallino, R., "Neutron-Capture Elements in the Early Galaxy", *Annual Review of Astronomy and Astrophysics*, **46**, 241, (2008).

Sneden, C., Cowan, J. J., Lawler, J. E., et al., "The Extremely Metal-poor, Neutron Capture-rich Star CS 22892-052: A Comprehensive Abundance Analysis", *Astrophysical Journal*, **591**, 936, (2003).

Suzuki, T. K., & Nagataki, S., "Alfvén Wave-driven Proto-Neutron Star Winds and r-Process Nucleosynthesis", *Astrophysical Journal*, **628**, 914, (2005).

Symbalisty, E. M. D., "Magnetorotational iron core collapse", *Astrophysical Journal*, **285**, 729, (1984).

Takiwaki, T., & Kotake, K., "Gravitational Wave Signatures of Magnetohydrodynamically Driven Core-collapse Supernova Explosions", *Astrophysical Journal*, **743**, 30, (2011).

Takiwaki, T., Kotake, K., Nagataki, S., & Sato, K., "Magneto-driven Shock Waves in Core-Collapse Supernovae", *Astrophysical Journal*, **616**, 1086, (2004).

Takiwaki, T., Kotake, K., & Sato, K., "Special Relativistic Simulations of Magnetically Dominated Jets in Collapsing Massive Stars", *Astrophysical Journal*, **691**, 1360, (2009).

Tanaka, M., & Hotokezaka, K., "Radiative Transfer Simulations of Neutron Star Merger Ejecta", *Astrophysical Journal*, **775**, 113, (2013).

Tanvir, N. R., Levan, A. J., Fruchter, A. S., et al., "A 'kilonova' associated with the short-duration γ-ray burst GRB 130603B", *Nature*, **500**, 547, (2013).

Tatsuda, S., Yamamoto, K., Asano, T., et al., "Fission modes of neutron-rich nuclei in the r-process nucleosynthesis", in *American Institute of Physics Conference Series*, Vol. 1016, *Origin of Matter and Evolution of Galaxies*, ed. T. Suda, T. Nozawa, A. Ohnishi, K. Kato, M. Y. Fujimoto, T. Kajino, & S. Kubono, 469–471, (2008).

Terasawa, M., Sumiyoshi, K., Kajino, T., Mathews, G. J., & Tanihata, I., "New Nuclear Reaction Flow during r-Process Nucleosynthesis in Supernovae: Critical Role of Light, Neutron-rich Nuclei", *Astrophysical Journal*, **562**, 470, (2001).

Thielemann, F.-K., Arcones, A., Käppeli, R., et al., "What are the astrophysical sites for the r-process and the production of heavy elements?", *Progress in Particle and Nuclear Physics*, **66**, 346, (2011).

Thompson, T. A., Quataert, E., & Burrows, A., "Viscosity and Rotation in Core-Collapse Supernovae", *Astrophysical Journal*, **620**, 861, (2005).

Trippella, O., Busso, M., Maiorca, E., Käppeler, F., & Palmerini, S., “s-Processing in AGB Stars Revisited. I. Does the Main Component Constrain the Neutron Source in the ^{13}C Pocket?”, *Astrophysical Journal*, **787**, 41, (2014).

Tsujimoto, T., & Shigeyama, T., “Enrichment history of r-process elements shaped by a merger of neutron star pairs”, *Astronomy and Astrophysics*, **565**, L5, (2014a).

—, “The Origins of Light and Heavy R-process Elements Identified by Chemical Tagging of Metal-poor Stars”, *Astrophysical Journal Letters*, **795**, L18, (2014b).

Valentim, R., Rangel, E., & Horvath, J. E., “On the mass distribution of neutron stars”, *Monthly Notices of the Royal Astronomical Society*, **414**, 1427, (2011).

van de Voort, F., Quataert, E., Hopkins, P. F., Kereš, D., & Faucher-Giguère, C.-A., “Galactic r-process enrichment by neutron star mergers in cosmological simulations of a Milky Way-mass galaxy”, *Monthly Notices of the Royal Astronomical Society*, **447**, 140, (2015).

Vlasov, A. D., Metzger, B. D., & Thompson, T. A., “Neutrino-heated winds from rotating protomagnetars”, *Monthly Notices of the Royal Astronomical Society*, **444**, 3537, (2014).

Wanajo, S., “The r-process in Proto-neutron-star Wind Revisited”, *Astrophysical Journal Letters*, **770**, L22, (2013).

Wanajo, S., Janka, H.-T., & Müller, B., “Electron-capture Supernovae as The Origin of Elements Beyond Iron”, *Astrophysical Journal Letters*, **726**, L15, (2011).

Wanajo, S., Sekiguchi, Y., Nishimura, N., et al., “Production of All the r-process Nuclides in the Dynamical Ejecta of Neutron Star Mergers”, *Astrophysical Journal Letters*, **789**, L39, (2014).

Wasserburg, G. J., Busso, M., & Gallino, R., “Abundances of Actinides and Short-lived Non-actinides in the Interstellar Medium: Diverse Supernova Sources for the r-Processes”, *Astrophysical Journal Letters*, **466**, L109, (1996).

Watanabe, H., Lorusso, G., Nishimura, S., et al., “Isomers in Pd128 and Pd126: Evidence for a Robust Shell Closure at the Neutron Magic Number 82 in Exotic Palladium Isotopes”, *Physical Review Letters*, **111**, 152501, (2013).

Wehmeyer, B., Pignatari, M., & Thielemann, F.-K., “Galactic evolution of rapid neutron capture process abundances: the inhomogeneous approach”, *Monthly Notices of the Royal Astronomical Society*, **452**, 1970, (2015).

Wilkins, B. D., Steinberg, E. P., & Chasman, R. R., “Scission-point model of nuclear fission based on deformed-shell effects”, *Physical Review C*, **14**, 1832, (1976).

Winteler, C., Käppeli, R., Perego, A., et al., "Magnetorotationally Driven Supernovae as the Origin of Early Galaxy r-process Elements?", *Astrophysical Journal Letters*, **750**, L22, (2012).

Woosley, S. E., & Heger, A., "The Progenitor Stars of Gamma-Ray Bursts", *Astrophysical Journal*, **637**, 914, (2006).

Woosley, S. E., Wilson, J. R., Mathews, G. J., Hoffman, R. D., & Meyer, B. S., "The r-process and neutrino-heated supernova ejecta", *Astrophysical Journal*, **433**, 229, (1994).

Yang, B., Jin, Z.-P., Li, X., et al., "A possible macronova in the late afterglow of the long-short burst GRB 060614", *Nature Communications*, **6**, 7323, (2015).